Journal of the Institute of Petroleum

VOL. 40 APRIL 1954 No. 364

CONTENTS

Redwood Lecture: The Friction of Non-metallic Solids

By F. P. Bowden

A Method for Approximate Determination of Viscosity–Pressure–Temperature Relationships for Oils

By Sven Lundberg

Viscosity as a Means in the Graphical Statistical Analysis of Mineral Oils

By C. Boelhouwer and H. I. Waterman

Comparison of Viscosities of American Grades of Cutback Bitumens

By C. M. Gough

Abstracts 404-557

Book Review

Additions to Library

PRICE 10s 0D A COPY OR

£4-14-6 YEARLY *POST FREE*

Published by the Institute of Petroleum 26 Portland Place London W1

Printed in Great Britain by Richard Clay and Company Ltd Bungay Suffolk

COUNCIL, 1953–54

President

H. S. Gibson, C.B.E., M.A., M.I.Mech.E.

Past-Presidents

Sir Andrew Agnew, C.B.E.
S. J. M. Auld, O.B.E., M.C., D.Sc.
T. Dewhurst, A.R.C.S.
A. E. Dunstan, D.Sc., F.R.I.C.
E. A. Evans, M.I.Mech.E., F.R.I.C.
F. H. Garner, O.B.E., Ph.D., F.R.I.C.
C. A. P. Southwell, C.B.E., M.C., B.Sc.

Vice-Presidents

E. B. Evans, M.Sc., Ph.D., F.R.I.C.
H. Hyams
J. A. Oriel, C.B.E., M.C., M.A., B.Sc., F.R.I.C., M.I.Chem.E.
H. E. F. Pracy, B.A., M.I.Chem.E.
R. B. Southall, C.B.E.
G. H. Thornley, M.Sc.

Members of Council

W. S. Ault, B.A.
V. Biske, B.Sc., LL.M., F.R.I.C.
C. D. Brewer, M.I.Mech.E.
E. J. Dunstan, M.Sc., M.I.Chem.E.
F. L. Garton, M.A., B.Sc.
A. J. Goodfellow, B.Sc., A.R.I.C.
A. C. Hartley, C.B.E., F.C.G.I., B.Sc.(Eng.), M.I.C.E., M.I.Mech.E.
E. LeQ. Herbert, B.Sc., F.R.I.C.
E. C. Masterson, B.Sc.
F. Morton, Ph.D., D.Sc., F.R.I.C.
J. S. Parker, M.A., B.Sc.
A. J. Ruthven-Murray, M.A., B.Sc.
D. L. Samuel, B.Sc., A.R.I.C.
G. H. Smith, Ph.D.
A. R. Stark, B.Sc., A.R.I.C.
E. J. Sturgess, B.Sc.
W. H. Thomas, A.R.S.M.
O. F. Thompson, O.B.E.
A. T. Wilford, B.Sc., F.R.I.C.
C. G. Williams, D.Sc., M.I.Mech.E., F.R.Ae.S.
C. S. Windebank, B.Sc., M.S.

Ex-Officio

S. A. Berridge, Fawley Branch
A. W. Deller, D.F.C., London Branch
H. H. Ballard, Northern Branch
E. J. Horley, South Wales Branch
W. M. Stirling, A.H-W.C., A.M.I.E.E., Scottish Branch
N. W. Grey, South-Eastern Branch

Honorary Secretary

C. Chilvers, B.Sc., F.R.I.C.

Honorary Treasurer

G. H. Coxon

General Secretary

D. A. Hough, F.I.A.C.

Honorary Editor

F. H. Garner, O.B.E., Ph.D., F.R.I.C.

Honorary Associate Editor

E. B. Evans, M.Sc., Ph.D., F.R.I.C.

Editor

George Sell

Honorary Secretaries of Branches

Fawley Branch: S. A. Berridge, c/o Esso Petroleum Co. Ltd., Fawley, Southampton.

London Branch: R. F. Leach, M.A., c/o Shell-Mex and B.P. Ltd., Shell-Mex House, Strand, London, W.C.2.

Northern Branch: G. M. Davies, c/o Esso Petroleum Co. Ltd., Mode Wheel Installation, Trafford Wharf Road, Manchester 17.

Persian Gulf Branch: G. A. Hoss, B.A., c/o Kuwait Oil Co. Ltd., Kuwait, Persian Gulf.

Scottish Branch: W. M. Stirling, A.H-W.C., A.M.I.E.E., Scottish Oils Ltd., Middleton Hall, Uphall, Broxburn, W. Lothian.

South-Eastern Branch: F. A. Maliphant, c/o Anglo-Iranian Oil Co. Ltd., Kent Oil Refinery, Isle of Grain.

South Wales Branch: E. J. Horley, National Oil Refineries Ltd., Llandarcy, Glam.

Stanlow Branch: V. Biske, B.Sc., LL.M., F.R.I.C., Lobitos Oilfields Ltd., The Refinery, Ellesmere Port, Cheshire.

Trinidad Branch: E. G. Everett, c/o United British Oilfields of Trinidad Ltd., Point Fortin, Trinidad, B.W.I.

VOL. 40 NO. 364 APRIL 1954

THE INSTITUTE OF PETROLEUM

REDWOOD LECTURE

A MEETING of the Institute was held at Manson House, Portland Place, W.1, on 2 December 1953, when Dr F. P. Bowden, ScD., F.R.S., delivered the Redwood Lecture and was presented with the Redwood Medal. Mr H. S. Gibson, C.B.E., president, was in the Chair, and opening the meeting said:

It is my privilege this evening to introduce Dr Bowden, a distinguished scientist from Cambridge, who has devoted a great deal of attention and of his skill as a physicist to a subject which is of special interest to those of us who are concerned with lubrication. I shall have more to say about Dr Bowden at a ceremony which it will be my pleasant duty to perform at the conclusion of his lecture; so without further delay I will now ask him to deliver his Redwood Lecture on "The Friction of Non-metallic Solids."

THE FRICTION OF NON-METALLIC SOLIDS

By F. P. BOWDEN,* Sc.D., F.R.S.

CONTENTS

Friction of metals.
Use of reflection electron microscopy.
Friction of non-metals:
(*a*) Plastic solids; (*b*) Brittle solids; (*c*) Elastic solids; (*d*) Snow and ice; (*e*) Solid krypton; (*f*) Molecularly flat surfaces.

IN looking through earlier lectures given by my predecessors I have been struck not only by the distinction of the speakers but also by the wide variety of the lectures they have given. It is clear that no rigid framework is laid down by the Institute, and I thought that on this occasion instead of giving a general review of our past work I would discuss some of the recent experimental work which our laboratory has been doing in its further study of the friction of solids. Much of this has not yet been published, so that my talk must be somewhat scrappy and unpolished—I ask your indulgence on this.

There is no need to remind this audience of the two experimental laws of friction. First, that friction F is independent of the area of the surface, and second, that it is proportional to the load W. This means that the coefficient of friction $\mu = F/W$ is a constant. The first formulation, which I have found, of these laws is due to Leonardo da Vinci, but it was the French engineer, Amontons, who established them experimentally some 200 years later in 1699.

I would like first to remind you very briefly of the general physical picture we have for the friction of metals and then to go on to deal mainly with the behaviour of non-metallic solids. In particular, I would like to discuss the behaviour of plastic, brittle, and elastic solids.

THEORY OF METALLIC FRICTION

We now have a good deal of evidence that one of the major factors responsible for metallic friction is the adhesion which occurs in the regions of local contact. We have been using a variety of physical methods for studying the surface topography and surface contour of solids. All these methods show that even if solids are carefully prepared and polished their surfaces are never flat, so that when two solids are put together the top surface will be supported on the summit of the highest irregularities, and the area in intimate contact will be small. Detailed measurements show that the area is indeed very small; it varies with the load, but for flat steel surfaces may be less than one ten-thousandth part of the apparent area.

The experiments are also interesting in that they show that the real area of contact is almost independent of the size of the surface. It is also very little influenced by the shape and degree of roughness of the surfaces; it depends mainly on the load which is applied to them, and is, in fact, directly proportional to the load. The general behaviour is consistent with the view that the surfaces are held apart by small irregularities (see Fig 1). This means that, even with lightly loaded surfaces, the local pressure at these small points of contact is very high and may be sufficiently great to cause the hardest metals to flow plastically.

Although the stresses will cause elastic deformation of the metal in the vicinity of the points of contact, the experiments suggest that the summits of irregularities on which the bodies are supported flow plastically and are crushed down until their cross-section is sufficient to enable them to support the applied load. The real area of contact A is given by $A = W/p_m$, where p_m is the yield pressure of the metal.

The fact that the real area of contact is so small has important practical implications. Even when loads of only a few grams are applied to the surfaces, the local pressure between them may be sufficiently great to cause the flow of metal. When large flat surfaces are used, it does not mean that the real pressure is much less, but merely that the points of

* Research Laboratory for the Physics and Chemistry of Surfaces, Department of Physical Chemistry, University of Cambridge.

contact are more widely distributed. This intense pressure will cause adhesion or "pressure welding" at the tiny points of contact and so produce small metallic junctions between the surfaces.

There is strong evidence that the friction of metals is due, in a large measure, to these localized adhesions and represents the force necessary to shear these small junctions. As a rough approximation we may therefore write $F = As$, where s is the shear strength of the junctions. In addition to this the surface irregularities of the harder metal may penetrate the surface of the softer one and work may be required to plough out a track in the path of the slider. If the metals are of similar hardness and the configuration of the surfaces is suitable some interlocking of the surface irregularities may also occur. Experiment shows that these effects are usually small compared with the shearing term, and may under many conditions of sliding be neglected.

We see that this picture offers a simple explanation of the two laws of friction. First, since A, the real area of intimate contact, is independent of the size of the surfaces, the friction will be independent of it. Secondly, since the real area of contact A is proportional to the load the friction will be too. For the above reasons we may expect the friction of most metals (and indeed of most plastic solids) to have a similar value. A soft solid gives a large A but a small s, and a hard solid a small A but a large s.

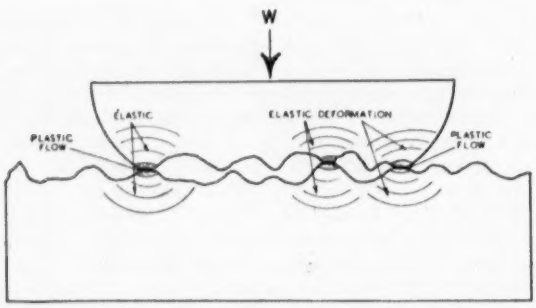

FIG 1

TWO SOLIDS PLACED IN CONTACT ARE SUPPORTED ON THE SUMMITS OF SURFACE IRREGULARITIES

The pressure exceeded the yield pressure p_m of the solid, which flows plastically until the area of contact A is sufficient to support the load W. Hence $A = W/p_m$. The material around the regions of contact will be elastically deformed. If s is the shear strength of the junctions, the friction $F = As$.

On occasion the shearing may occur at the interface, but more frequently (because of work hardening of the contact region) it occurs a little distance beyond it. A metal fragment is detached from one of the surfaces and wear occurs.

FRICTION OF CLEAN SURFACES

An important point to bear in mind here is that metals, and indeed most solids exposed to the air, will have a layer of oxide or of adsorbed gas on the surface. One usually breaks through these films, but they play an important part in reducing the extent of the metallic contact and in particular of

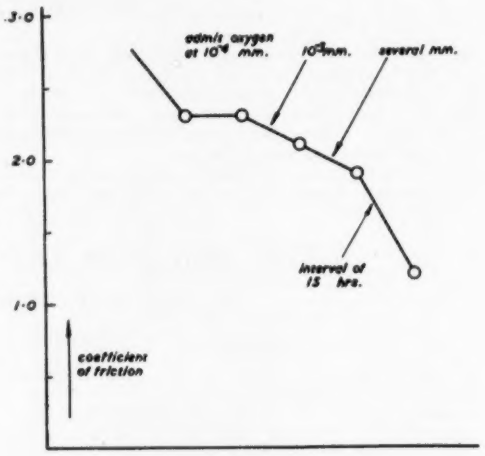

FIG 2

THE FRICTION OF REALLY CLEAN METAL SURFACES *IN VACUO* IS SO HIGH THAT SEIZURE OCCURS

When a trace of air or oxygen is admitted friction falls to the usual value.

reducing the growth of the welded junctions when sliding starts. If we take these surface films off the metal in a high vacuum, then we find that we cannot slide the metals at all. The metallic junctions grow to a large size, friction rises to a very high value, gross seizure occurs, and sliding is impossible. It is only when we admit air that the friction falls to the usual value (see Fig 2).

I will mention later some of the factors which influence the growth of these metallic junctions, and most of my discussion will deal with solids which are exposed to the air.

METALLIC TRANSFER BETWEEN SLIDING METALS

The reality of these localized adhesions may be shown in a number of ways. Fig 3 (*a*) and (*b*) shows taper sections cut from a steel surface after a copper slider has passed over it once. The localized welding of the copper on to the steel may be clearly seen. Another simple but very sensitive method of measuring this quantitatively is to use as a slider an artificially radio-active metal. If localized adhesion takes place, small fragments of the radio-active metal will be welded on the other surface and we may detect their presence either by a Geiger counter or an autophotographic method. Fig 4 shows an experiment, made by Dr Tabor and Dr Rabinowicz, in which a hemispherical piece of radio-active copper is placed

first on top of a flat copper surface in air, and is then taken away again without any sliding. The amount of radio-active copper welded on to the lower surface is about 10^{-10} g. If we allow sliding to occur the amount of metal transferred is enormously increased and the amount of copper transferred to the lower surface is now approximately 10^{-6} g/cm of track. There are two factors which are responsible for this increase. The first is the increased breakdown of the oxide film caused by sliding, and the second is the increase in the size of the metallic junctions when they are subjected to shear.

Recently E. Eisner has investigated the way in which the force resisting sliding builds up before

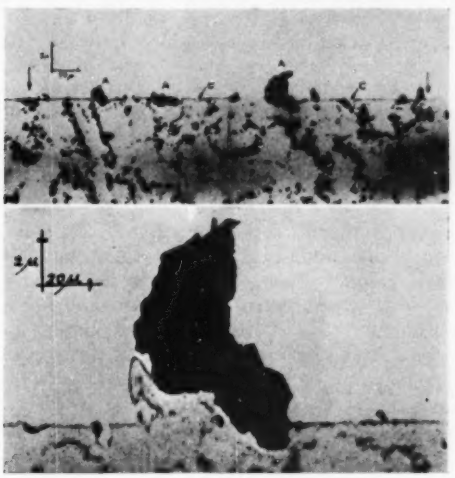

(*a*)

(*b*)

FIG 3

(*a*) TAPER SECTION OF STEEL SURFACE AFTER COPPER SLIDER HAS PASSED OVER IT ONCE

Tiny fragments of copper (dark) are welded on to the steel.

(*b*) DETAIL OF WELDED JUNCTION SHOWING COPPER FRAGMENT (DARK)

The copper has sheared at some distance from the interface.

sliding begins. He measured by optical interference methods the minute displacements which occur between bodies in contact when the tangential force is increased from zero to the full value necessary to produce gross sliding. Simultaneously the electrical resistance, which is a measure of the area of contact, has been measured. I would emphasize that these measurements are made before any slip occurs. There are two striking observations: first, even the smallest tangential forces produce measurable displacements; second, a large part of these displacements is irreversible, that is it is not associated with an elastic deformation. With oxide-free surfaces, such as gold or platinum, these displacements are accompanied by a continuous fall in electrical resistance which is also irreversible. For platinum surfaces at a load of 1 kg (see Fig 5) the resistance falls to about one-fifth of its initial value, showing that the area of intimate contact has greatly increased as a result of the displacement. The act of sliding

FIG 4

TRANSFER OF RADIO-ACTIVE COPPER ON NORMAL CONTACT

No sliding. Amount transferred c. 10^{-10} g.

(or of attempting to slide) produces a large increase in the metallic welding.

When the metal is covered with an oxide film irreversible changes of the same type occur for the smallest tangential forces. However, the electrical resistance shows an enormous drop during these minute displacements. For example, the results for

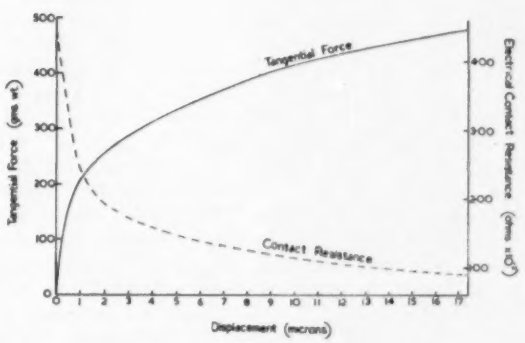

FIG 5

GROWTH OF TANGENTIAL FORCE WITH DISPLACEMENT BEFORE SLIDING OCCURS

Noble metal (platinum on platinum). As the tangential force rises, the metallic junctions grow in area and the contact resistance decreases.

mild steel surfaces are shown in Fig 6, where the resistance has been plotted on logarithmic co-ordinates; it is seen that it falls to about one three-hundredth of its initial value during a displacement of less than 10^{-4}

cm. This is primarily due to penetration and rupture of the oxide films so that the metallic junctions can be formed. If a lubricant is placed on the surfaces (lower curve, Fig 6), the lubricant film protects the oxide film, breakdown is inhibited, the metallic junctions do not grow, and the electrical resistance remains relatively high.

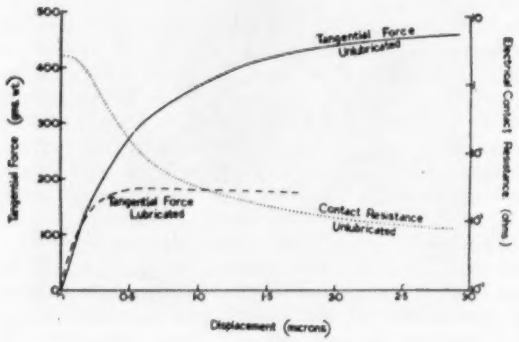

FIG 6

GROWTH OF TANGENTIAL FORCE WITH DISPLACEMENT BEFORE SLIDING OCCURS

Results for mild steel. Again the contact resistance decreases as the tangential force is increased but the effect is very much greater because of the progressive breakdown of the oxide layer. Lubrication inhibits this and hinders junction growth.

METALLIC TRANSFER IN SCREWING AND BOLTING

This metallic transfer is of fundamental importance in friction, lubrication, and wear, but it may also be significant in other affairs—even possibly to you if you break a leg. In modern surgery it is customary to use metallic plates to strengthen or to replace a bone fracture. These are screwed or bolted on to the bone and remain permanently in position. The insertion of "mixed metals" is always avoided since the presence of an "electrolytic couple" causes inflammation of the tissue. The plates, screws, and bolts are all made from the same stainless steel which has a very high corrosion resistance. Nevertheless, it is found in practice that inflammation does occasionally occur. This is usually accompanied by corrosion and iron is found in the surrounding tissue.

Although the screws and plates are all made from the same steel, the tools for handling them, *i.e.* the screwdrivers and spanners, are made from a different steel which is less resistant to corrosion. If small fragments of this different steel are welded on to the screws during the screwing operation they may, when immersed in the body tissue, form small electrolytic couples, which may cause inflammation and accelerate corrosion. In collaboration with Patrick Gowans Laing, F.R.C.S., and J. B. P. Williamson, a preliminary investigation has been made to see whether such a metallic transfer occurs. The tip of the screwdriver was first made artificially radio-active by treatment in the pile at Harwell, and was then used to drive the screws into bone in the normal way. The screw heads were then examined for radio-activity. The results are shown in the following table:

TABLE I

Amount of Metal Transferred from Driver to Screw

	μg
Driven carefully . . .	22
Slight slip	47
Greater slip	65
Extreme care . . .	17

It is clear than an appreciable amount of metal is transferred from the driver to the screw, and this amount increases with the force used. An autoradiograph (Fig 7 (*a*)) of the screw head showed that the pick-up metal consisted of a small number of discrete particles distributed along the outer edges of the slot of the screw (see Fig 7 (*b*)). Electropotential measurements showed that the adhering metal is strongly electronegative to the metal of the screw so that an electrolytic couple could be set up. The difficulty might perhaps be overcome by making the tools from the same material as the screws and bolts.

This work is still in the early stages. It is interesting to note that such metallic transfer occurs whenever we perform a simple mechanical operation like screwing and bolting.

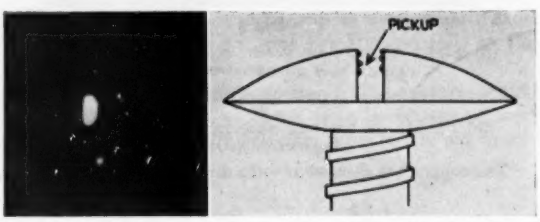

(*a*) (*b*)

FIG 7

(*a*) AUTORADIOGRAPH OF SCREW HEAD SHOWING TRANSFER OF METAL FROM THE SCREWDRIVER

(*b*) DISTRIBUTION OF METALLIC PICKUP ON SCREW

Now I would like to discuss the behaviour of some non-metallic solids: first, a plastic solid (we will consider the behaviour of some polymerized "plastics"); second, a brittle solid, like rock-salt or glass; and, third, an elastic solid, like diamond. I propose to show that the general mechanism of friction for these solids is similar to that for metals, but there are important and interesting differences.

REFLECTION ELECTRON MICROSCOPY

Before discussing this subject, I would like to mention a new technique which is proving of great value to us, that is the development of reflection electron microscopy. The development of this in our laboratory is due mainly to Dr J. W. Menter with the assistance of Dr J. S. Courtney-Pratt.

The electron microscope is, of course, a very powerful instrument for studying the detailed structure of surfaces. It normally works by transmission, and it is generally necessary to prepare transparent replicas of the surfaces. Apart from the fact that replica techniques are often a tricky business, it is never certain that they follow the original contour

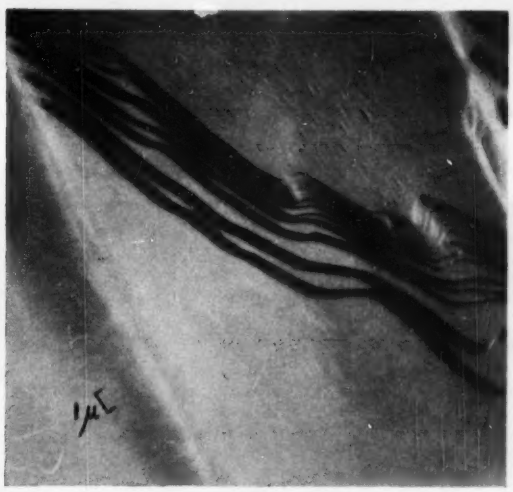

FIG 8

REFLECTION ELECTRON MICROGRAPH OF CLEAVAGE STEPS ON A MICA SURFACE

exactly, nor is the interpretation of the transmission micrograph obtained from the replica always unequivocal. These difficulties do not arise when the electron microscope is used as a reflection instrument. The general principle is to direct the electron beam at glancing incidence on to the surface under examination, and to focus the scattered electrons in the usual way. Active work on this is being done in the U.S.S.R., in Germany, and in the U.K. The resultant electron micrograph reveals the surface contours somewhat in the same way as a pedestrian sees the surface irregularities of a road illuminated by oncoming car headlights. Long shadows are cast by surface irregularities, but they are foreshortened because of the small angle of viewing. It is, however, not difficult to calculate the true heights of the surface features revealed. The great advantage of this technique is that replicas are not necessary: the surface itself is examined directly by the beam.

Menter was the first to show that very simple modifications to a standard transmission microscope (Metropolitan-Vickers E.M.3) would enable it to take reflection micrographs of great clarity, high resolution, and considerable depth of focus.

A typical photograph obtained using this technique is reproduced in Fig 8. It shows a group of cleavage steps on a mica surface, the total height of the terrace being about 8000 Å. It is easily possible to resolve some steps as small as 100 Å in this terrace. A great advantage of the method is that the image has a considerable depth of field normal to the specimen surface. The unusual angle of illumination reveals the true character of such a feature in a very direct way. The high depth of field also permits the examination of relatively rough surfaces provided the asperities are not too large nor too closely spaced.

The method is proving extremely valuable in our studies of the damage produced by sliding one surface on another. Fig 9 (*a*) shows a track produced on a highly polished copper surface by a hemispherical steel slider with a load of 0·5 g. The saw-tooth effect in the track is due to stick–slip motion on a small scale, and is shown up particularly clearly on account of the oblique angle of viewing the surface. Fig 9 (*b*) shows a track produced with the same materials but with a load of 20 g. The high depth of field allows us to obtain a focused image of both the bottom and top of the track simultaneously.

Another interesting application has been in connexion with the cutting and turning of metals. During the past few years Sir Thomas Merton's new method of making optical diffraction grating replicas has been developed by Dr L. A. Sayce at the National Physical Laboratory. A virtually ghost-free master grating is obtained by turning on a cylinder using the Merton nut. The next few figures illustrate the character of experimental rulings obtained by Dr Sayce and his collaborators on a 1-inch diameter aluminium cylinder, using a 90° diamond as a cutting tool to make a one-thousand turns-per-inch ruling. In this particular case the tool was set at an angle of 15° to the axis of the cylinder in order to produce a grating with a 15° blaze. Fig 10 shows the ruling produced with an inadequate load on the tool. The action of the diamond is not in fact a cutting action. It has merely pushed the aluminium to one side during its passage. Note the remarkable smoothness of the surface over which the diamond tool has passed compared with that of the virgin lapped surface.

A further check on the groove profile may be obtained by examining the silhouette image of the edge of the cylinder in the transmission electron microscope. Fig 11 shows the silhouette image corresponding to the reflection image shown in the previous slide. Here again we can see where the tool has passed and how it has thrown up a parapet of aluminium to one side of the track. Fig 12 is a reflection micrograph of a grating produced with a heavier load on the tool. Here the profile of the grating is much better as the tool has carried away the parapet of aluminium during its next passage

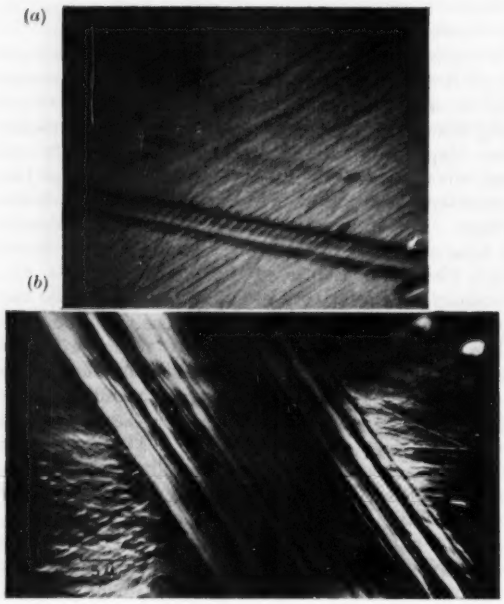

FIG 9

(*a*) REFLECTION ELECTRON MICROGRAPH OF TRACK ON POLISHED COPPER AT LIGHT LOAD 0·5 G

(*b*) ANALOGOUS TRACK AT HEAVIER LOAD 20 G

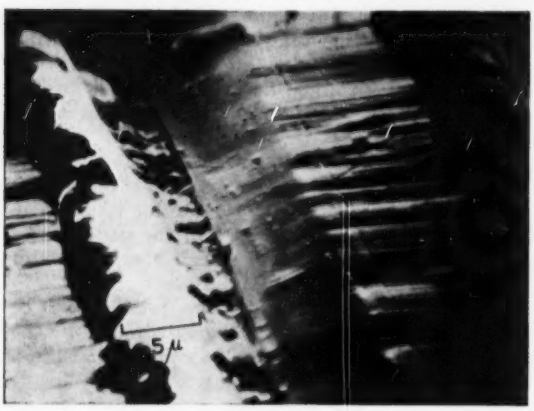

FIG 10

REFLECTION ELECTRON MICROGRAPH OF CUT MADE IN ALUMINIUM BY DIAMOND TOOL SET INCORRECTLY

Note pile up of metal.

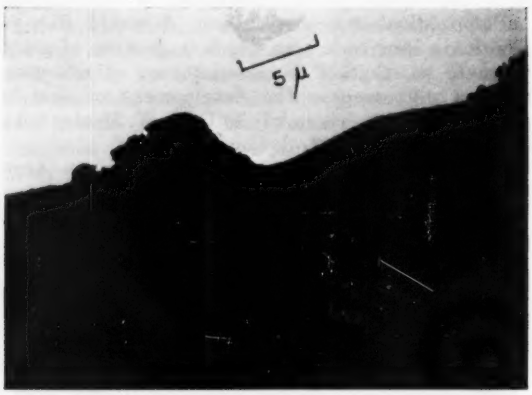

FIG 11

CORRESPONDING SILHOUETTE ELECTRON MICROGRAPH SHOWING IMPERFECT CONTOUR

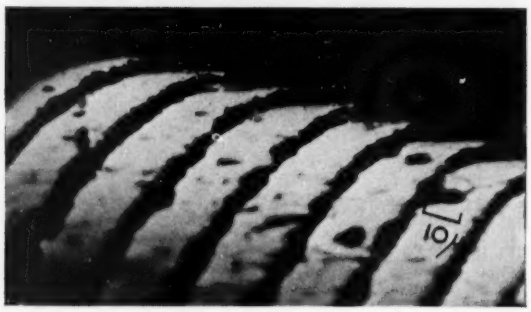

FIG 12

REFLECTION ELECTRON MICROGRAPH OF CUT MADE IN ALUMINIUM BY DIAMOND TOOL; IMPROVED CUTTING

FIG 13

CORRESPONDING SILHOUETTE ELECTRON MICROGRAPH OF IMPROVED CUTTING

around the cylinder. This is again confirmed by the silhouette image of the edge of the cylinder (Fig 13).

It is clear that reflection electron microscopy is providing us with a new and useful tool for studying these problems.

Now let us return to our task of considering the friction of plastic, brittle, and elastic solids.

PLASTIC SOLIDS

The Friction of "Plastics"

A study of the behaviour of a group of structurally related synthetic polymers has been made by Dr D. Tabor, Dr K. V. Shooter, and Dr R. F. King. Again there is strong evidence for localized adhesion in the regions of contact. Fig 14 shows the track formed when a slider of polyvinyl chloride has passed once over a surface of the same material. The material from the slider is welded on to the lower surface. A similar effect is observed when the plastic slides on a metal (Fig 15) or indeed when a metal slides on a plastic (Fig 16). Some typical values of the friction for a number of plastics are given in Table II.

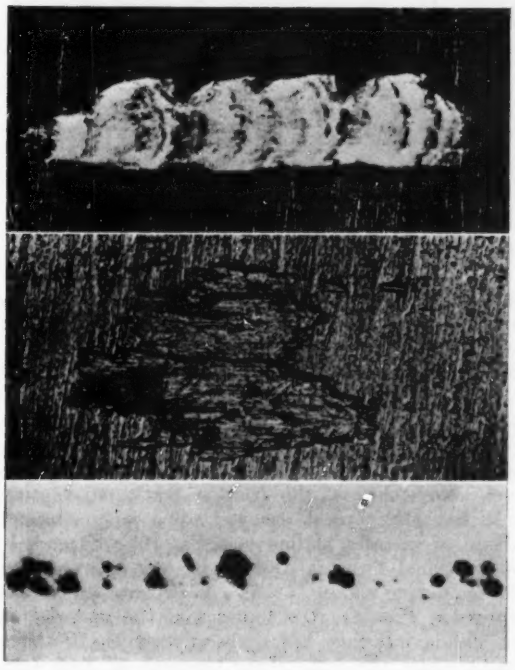

FIG 14

TRACK FORMED WHEN POLYVINYL CHLORIDE SLIDES ON ITSELF
Welding occurs. × 30.

FIG 15

TRACK FORMED WHEN POLYVINYL CHLORIDE SLIDES ON STEEL
The plastic is welded on to the steel. × 200.

FIG 16

TRACK FORMED WHEN RADIO-ACTIVE SILVER SLIDES ON POLYVINYL CHLORIDE

Some metal (*c.* 3×10^{-8} g/cm of track) is transferred to the plastic. × 10.

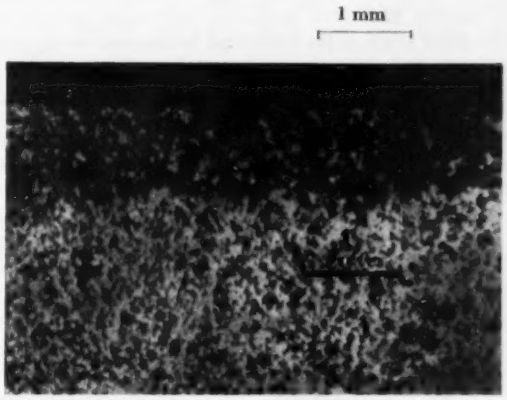

FIG 17

POROUS COPPER WITH THE SURFACE LAYERS IMPREGNATED WITH P.T.F.E.

This has the mechanical and thermal properties of sintered copper combined with the low friction of P.T.F.E.

TABLE II
Friction of Plastics

Plastics	Coefficient of friction, μ
Polyvinyl chloride (P.V.C.)	0·4 to 0·5
Polymethyl methacrylate (Perspex)	0·4 to 0·5
Polystyrene	0·4 to 0·5
Nylon	0·3
Polyethylene (Polythene)	0·5 to 0·8
Polytetrafluoroethylene (P.T.F.E.)	0·05 to 0·1

Mechanism of friction is similar to that for metals. The area of contact A is proportional to the load and the friction $F = As$, where s is roughly equal to the shear strength of the plastic itself.

Note the exceptionally low friction for P.T.F.E.

With loads heavier than a few grams the area of contact A is proportional to the load. The friction is again given by $F = As$, where s is roughly equal to the shear strength of the plastic itself. In addition, it is found that the coefficient of friction is independent of the load. It is clear that the mechanism of friction for these materials is essentially the same as that for metals.

At light loads (below a few grams) the behaviour is different. The coefficient of friction is no longer constant, but increases as the load decreases. There is evidence that, at light loads, some elastic deformation of the contact regions may occur (see below).

An interesting point of some importance to be noted from Table II is that polytetrafluoroethylene (P.T.F.E.) gives an extremely low friction. It is clear that the adhesion over the regions of contact

at the surface of this material is remarkably small. This appears to be a characteristic of the material itself, since even in a high vacuum when extraneous surface films are removed the friction remains low. It clearly has very desirable frictional properties. We have studied its frictional behaviour when it is incorporated in a porous metal such as sintered copper (Fig 17). In this way we have a material which possesses the mechanical and thermal properties of sintered copper but has the frictional properties of the plastic. Some typical values at different temperatures are given in Table III. This

TABLE III

Coefficient of Friction of Metal Impregnated with P.T.F.E.

Temp °C	Copper	Impregnated Copper
15	about 1·0	0·05
100	about 1·0	0·05
200	about 1·0	0·05
250	greater than 1	0·05

combination gives a very low friction ($\mu = 0{\cdot}05$), it is lower than the friction of a well lubricated surface, it maintains its properties up to high temperatures. It will, I think, prove a useful low friction material.

BRITTLE SOLIDS

The Friction of Rock-salt

So far we have been dealing with solids which are characterized by their ability to flow plastically

FIG 18

ELECTRON MICROGRAPH OF ROCK-SALT SURFACE AFTER SLIDING

Note fragmentation and tilting of small blocks.

without fracture. We may now ask what happens with brittle materials, such as rock-salt, glass, sapphire, and a vast number of minerals. Is a different mechanism of friction necessary for these substances?

Recently, Dr Tabor and Dr King have made a detailed study of the friction of rock-salt and similar

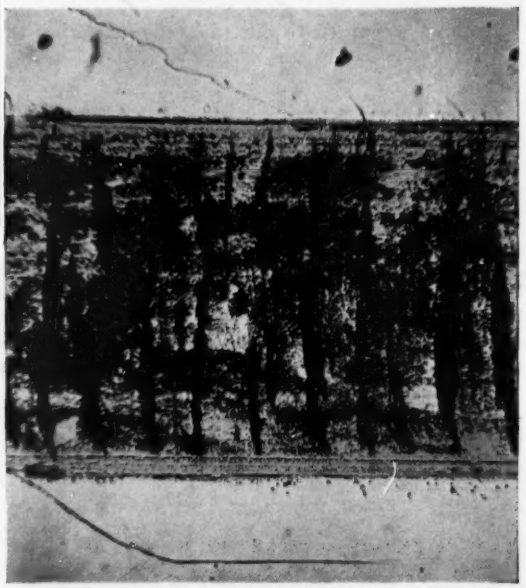

FIG 19

GROOVED TRACK MADE BY CURVED SLIDER ON ROCK-SALT

Plastic deformation has occurred. × 160.

materials. With rock-salt the coefficient of friction ($\mu = 0{\cdot}8$) is of the same order of magnitude as that obtained with metals. There are, however, two puzzling observations. First, the surface damage, as revealed by the electron microscope (Fig 18) shows that fragmentation of the surface, on a microcrystalline scale, has occurred, minute blocks of the rock-salt being tilted relative to the original surface level. Nevertheless, the friction track on a gross scale has the typical grooved appearance characteristic of metallic sliding (see Fig 19). Second, if the frictional force is divided by the area of real contact during sliding, *i.e.* if s is determined in the expression $F = As$, it is found that the material at the sliding interface has a shear strength 10 times greater than the bulk shear strength of rock-salt. Whatever the mechanism of friction this is an unexpected result.

This behaviour becomes explicable when it is realized that the material in the region of contact is under very high hydrostatic pressures. Independent compression experiments show that under these conditions rock-salt ceases to be brittle and can undergo marked plastic deformation, the stresses that the crystal can withstand before it yields plastically being many times higher than the stresses required to produce fracture in an uncompressed

specimen. Further, if two rock-salt specimens are pressed together between rigid anvils so that there is appreciable plastic flow, marked adhesion occurs between the crystals, and the interface is almost as strong as a single crystal. These compression experiments can be carried out between glass anvils, and it is then seen that the criss-cross cracks which traverse the crystal during the early stages of the compression are healed as the pressure is increased, brittle fracture is inhibited, and the rock-salt becomes relatively ductile (Fig 20).

These experiments explain the two observations discussed above. Although the friction track is accompanied by some cracking and surface fragmentation, the behaviour is dominated by plastic deformation of the surface layer. Secondly, because of the high hydrostatic pressures developed during sliding the interface is very much stronger than rock-salt in bulk. These results, and similar ones obtained with other brittle materials, suggest that the frictional behaviour of brittle solids is primarily due, as with metals, to local plastic flow and to strong interfacial adhesion at the regions of real contact.

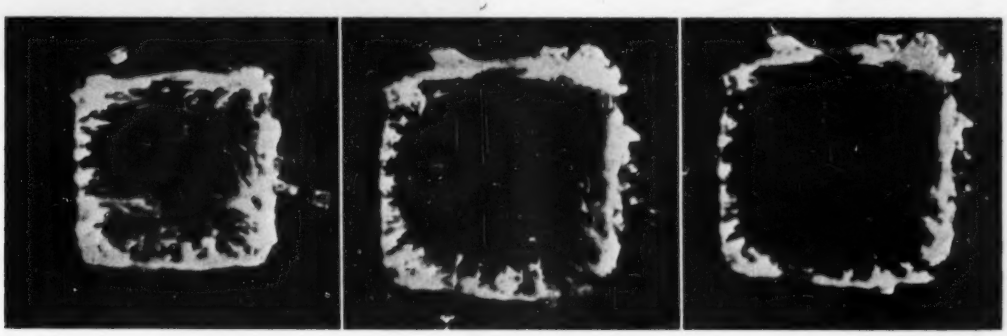

(a) (b) (c)

FIG 20

CRYSTAL OF ROCK-SALT SHOWING PROGRESSIVE HEALING OF CRACKS AS THE PRESSURE IS INCREASED. × 5

There is one marked difference between the friction of rock-salt and metals. If rock-salt is thoroughly cleaned by heating to a high temperature in a vacuum the gross seizure observed with metals does not occur. This is probably because any junction growth that occurs on the rock-salt reduces the average pressure, and so shifts the deformation properties towards the brittle range. Under these conditions junction growth on an appreciable scale is not possible.

ELASTIC SOLIDS

The Friction of Diamond

It is interesting to contrast this behaviour with that of a solid which deforms elastically. With a substance like rubber for example, where the deformation of the contact regions is elastic, we should expect that the real area of contact A would no longer be proportional to the load, W. Instead $A \propto W^{\frac{2}{3}}$. The coefficient of friction will no longer be constant, but will increase at light loads. This behaviour in fact is observed with rubber, and as we have seen it can occur with very low loads on "plastics."

It is also observed on diamond. Diamond is, of course, a very hard material, and we should expect the deformation in the contact region to be mainly elastic. This is illustrated by Fig 21. The lower curve shows the coefficient of friction of diamond in air plotted against load. It is not constant. It rises as light loads and is proportional to $W^{\frac{2}{3}}$. The deformation is apparently elastic.

A second effect, and an important one, which is shown in Fig 21, is the effect of putting the diamond in a vacuum and taking away the adsorbed film of oxygen and other gases which are normally present on the surface. With metals you will remember the effect was to cause an enormous rise in the friction and gross seizure. With diamond a similar effect is observed, although the effect is not quite so marked. The friction rises to a high value ($\mu = 0{\cdot}5$), and it is evident that the low friction ($\mu = 0{\cdot}05$), normally observed with diamond is due to adsorbed surface films. However, gross seizure does not occur, simply because the material is not ductile like a metal and junction growth cannot occur.

A calculation of the real area of contact, assuming elastic deformation and using Hertz's equation, shows that with clean diamonds the effective shear strength at the points of sliding contact is extremely high and is comparable with the bulk strength of diamond.

Although this part of the picture is clear, further work shows that the frictional behaviour of diamond is not simple.

We have seen that the deformation of the diamond is elastic. This is largely true, but recently M. Seal and Dr J. W. Menter, using reflection electron microscopy, have obtained evidence that some plastic deformation may occur during the polishing of

diamonds. Fig 22 shows a reflection electron micrograph of a diamond which has been polished in one direction only. The grooves formed by the diamond dust used for the polishing are apparent. Some fainter lines can be seen running at an angle to the polishing grooves. These lines follow the traces of octahedron planes, and these are the planes of greatest resolved shear stress; that is the direction along which slip would be most likely to occur. If

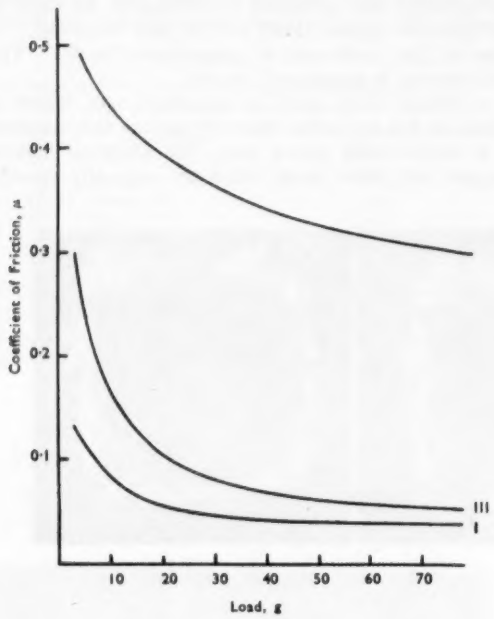

Fig 21

FRICTION OF DIAMOND

Curve I—Diamond exposed to the atmosphere. Curve II—Clean diamond in high vacuum. Curve III—Dry air admitted. Note that Amonton's Law is not obeyed.

this is so, the intense pressure at the points of contact of the polishing powder has produced plastic deformation of the diamond.

Also there is a directional effect. It is well known that the ease of polishing or grinding diamonds depends upon the orientation of the crystal face which is being worked. This is in accord with the crystalline structure. On the dodecahedral (110) face of a diamond the "soft" direction is that parallel to the crystal axis. Directions at right angles to this are hard, as Tolkowsky and later workers have shown. We might expect that the friction would be higher in the "soft" direction than in the "hard." Some preliminary results obtained by D. Kenyon for a hard diamond slider moving in different directions on a diamond crystal are shown in Fig 23. It was found that if the slider moved in a direction which was parallel to the crystal axis, the coefficient of friction ($\mu = 0{\cdot}5$) was several times greater than that observed in other directions ($\mu = 0{\cdot}04$).

Fig 22

REFLECTION ELECTRON MICROGRAPH OF A POLISHED DIAMOND SURFACE

Probable slip lines indicating plastic deformation are indicated by the arrow A. The polishing grooves follow the direction B.

These observations have an important bearing on the mechanism of wear of diamonds used in drilling, in dies for wire drawing, and in other practical operations.

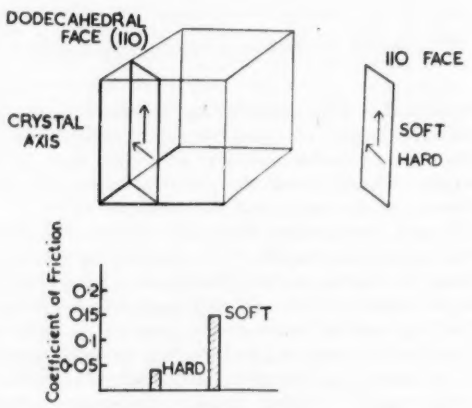

Fig 23

DIRECTIONAL EFFECT IN THE FRICTION OF DIAMOND CRYSTAL

Coefficient of friction in the "soft" direction is very much greater than that observed in the other directions.

FRICTION OF ICE AND SOLID KRYPTON

Finally, I would like to discuss the friction of a few solids which might appear to behave oddly. Let us consider first the behaviour of ice. It is an interesting

substance, since its friction can be lower by an order of magnitude than that of most other crystalline solids. The problem was discussed by Reynolds in about 1900, but he was rather diffident about it. He writes, " On trying to remember whether I had heard of any attempt to explain the slipperiness of ice in any way—for I felt at the moment as though everyone was laughing at me—I found that I could not recall any mention of the subject." He suggested that the low friction in skating is due to a water film formed by pressure-melting. I might perhaps mention with equal diffidence that my interest in friction problems and the decision to try a few experiments began when snow-bound in a mountain hut on a skiing expedition very many years ago. We had been able to ski reasonably fast on snow at −20° C, and it seemed highly improbable that pressure could produce melting at this temperature. Some years later in collaboration with Dr Hughes I made at the Jungfraujoch Research Station an experimental study of the friction of ice and snow. The friction of cold snow or ice is very high (see Fig 24). It is only at temperatures near 0° C that the friction is low. The experiments supported the view that

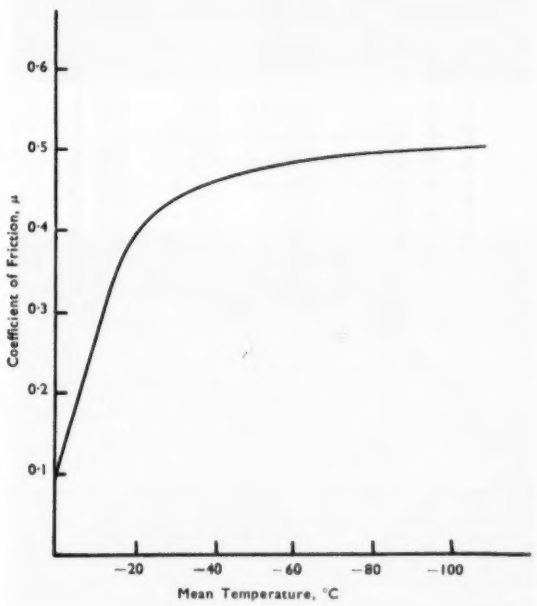

FIG 24

STATIC FRICTION ON ICE

On cold ice the friction is high. At temperatures near 0° C it falls to a low value.

the low friction is due to a surface melting. They showed, however, that pressure-melting is a factor only at temperatures very close to 0° C and with slow-moving surfaces. If the sliding speed is appreciable and temperatures are below 0° C the local surface melting is produced, not by pressure-melting, but by the frictional heating of the sliding surfaces. Under the conditions which obtain in skiing and

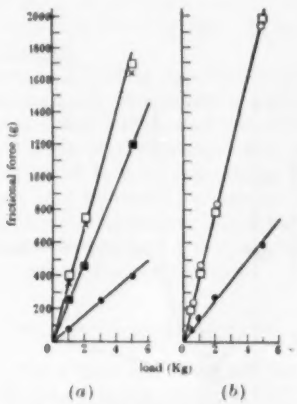

FIG 25

(*a*) FRICTION OF SMALL SLEDGES ON SNOW AT −10° C

□, Perspex, $\mu = 0{\cdot}34$; ×, Nylon, $\mu = 0{\cdot}30$; ■, Norwegian wax, $\mu = 0{\cdot}22$; ●, P.T.F.E., $\mu = 0{\cdot}08$.

(*b*) FRICTION OF SMALL SLEDGES ON SAND

□, Perspex, $\mu = 0{\cdot}4$; ○, ski lacquer, $\mu = 0{\cdot}4$; ●, P.T.F.E., $\mu = 0{\cdot}14$.

sledging it is this frictional heating and melting which is the major factor responsible for the low friction. Experiments with sliders of different thermal conductance were in harmony with this view. These early experiments were carried out with miniature sliders, at most a few centimetres in area.

Recently I have had an opportunity of extending this work to real skiing, and I would like to mention briefly some of these results and in particular to describe the behaviour of some plastic materials sliding on ice and snow.

The experiments supported the earlier conclusions that the low friction on snow and ice is due to a surface melting produced by the frictional heating of the sliding ski. The rubbing of the ski at the localized points of contact of the snow crystals causes a surface melting. At low temperatures the static friction of ice is high, and it is not until the ski begins to slide at an appreciable speed that the friction falls to a low value. This is illustrated in Table IV. Very cold snow or ice behaves like any other crystalline solid. Fig 25 (*a*) shows the static friction of a number of different surfaces sliding on snow at −10° C. It will be seen that the friction is proportional to the load, and the coefficient of friction (which is given by the slope of the line) is reasonably high for most solids. In fact, the friction of cold snow is very similar to the friction of dry sand. This is illustrated in Fig 25 (*b*). Note that P.T.F.E. gives the lowest friction of all these surfaces.

The influence of temperature on the friction of a

variety of surfaces sliding on snow is summarized in Fig 26. The two important points to be noted here are first that the friction for all these surfaces falls as the snow warms up, and is a minimum at 0° C when

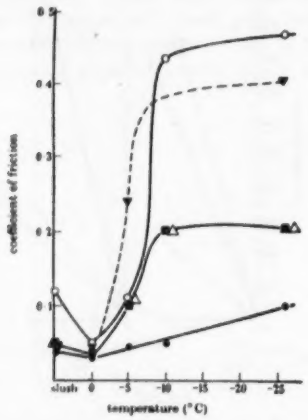

FIG 26

INFLUENCE OF TEMPERATURE ON THE STATIC FRICTION OF REAL SKI

○, ski lacquer; ▼, paraffin wax; ■, Norwegian wax; △, Swiss wax; ●, P.T.F.E.

surface melting can most readily occur. The second point to be observed is the very low friction given by P.T.F.E. under all conditions. I think that this behaviour of P.T.F.E. is due partly to its inherent good frictional properties (see above) and partly to the fact that it is not wetted by water. We have evidence that the frictional behaviour of different

TABLE IV

Influence of Speed on Friction : on Ice at −10° C

Ski surface	Coefficient of friction, μ		
	Static	at 3 cm/sec	at 5 m/sec
Waxed wood . . .	0·20	0·18	*c.* 0·02
Lacquered wood . .	0·40	0·36	*c.* 0·03
Perspex	0·35	0·32	*c.* 0·03
Aluminium . . .	0·38	0·34	*c.* 0·04

solids is influenced by the contact angle which the water film makes with the surface. With P.T.F.E. this contact angle is very high. This suggests that P.T.F.E. suitably applied may have interesting possibilities for skiers or at any rate for those skiers who like to ski fast. Some experiments with loaded skis were timed on snow slopes under various conditions, and it was found that the P.T.F.E. skis were faster than well waxed ones, and were considerably faster than skis coated with the standard lacquer.

THE FRICTION OF KRYPTON

We see that the friction of ice at temperatures well below the melting point is similar to the friction of metals and all other crystalline solids. G. W. Rowe has recently been examining the friction of solid krypton. The solids formed from the rare gases, such as krypton, argon, and neon, are held together by van der Waal forces which are weak compared with the bonding forces of metals. It might be thought that the surface fields of force, and hence the adhesion and friction of these solids, might be low. Measurements of the friction of solid krypton sliding on itself at c. −180° C show, however, that this is not so. This is illustrated in Fig 27. The static friction of solid krypton ($\mu = 0{\cdot}8$) is high, and similar to that of very cold ice or of rock-salt. At temperatures near the melting point or boiling point of krypton (these are very close together) the friction falls to a low value. This lubrication between the krypton surfaces is probably provided by the generation of gas and not liquid at the interface. Solid carbon dioxide behaves in a similar way. Its friction is high until the temperature is near the volatilization point, where it falls to a low value.

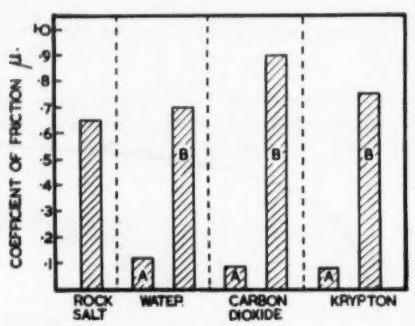

FIG 27

COMPARISON OF THE FRICTION OF SOLID WATER, CARBON DIOXIDE, AND KRYPTON WITH THAT OF ROCK-SALT

A—near solidification temperature; B—at temperature of liquid oxygen.

FRICTION BETWEEN MOLECULARLY FLAT SURFACES

In all previous experiments the surfaces have, on a molecular scale, been rough, so that contact has taken place only on the summits of the surface irregularities. For years we have been anxious to put some molecularly flat surfaces together and study their behaviour. Recently Miss Anita Bailey, who is working with Dr Courtney-Pratt, has been making some very beautiful experiments in which she achieves this. She is using thin sheets of cleaved mica, and by means of a very sensitive optical method she is able to determine whether the surfaces are molecularly flat or not.

Such surfaces are bent into the form of half cylinders and placed in contact with their axes at

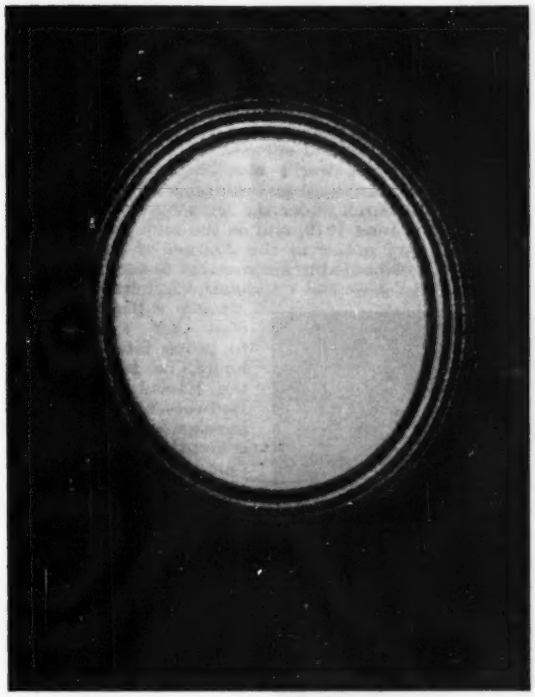

FIG 28

MICA SURFACES PLACED IN CONTACT

The surfaces are in molecular contact over the central region, and the diameter of this is 0·5 mm.

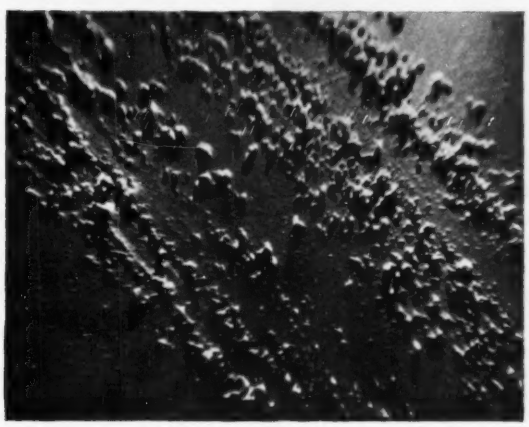

FIG 29

REFLECTION ELECTRON MICROGRAPH OF DAMAGE TO UNLUBRICATED MICA SURFACES WHICH HAVE BEEN IN MOLECULAR CONTACT

right angles. This gives a circular region of contact of known area where the two surfaces are within molecular distance. This is illustrated in Fig 28. The normal force required to separate them—that is the adhesion—or the tangential force required to slide them—that is the friction—can then be measured directly.

With clean mica surfaces exposed to the air the adhesion and friction are very high indeed, and the damage is profound (see Fig 29). It is rather like shearing solid mica.

A monolayer of lubricant can then be added to the surface. Immediately the adhesion and the friction fall to a much lower value, and when sliding takes place there is little or no damage over most of the area of contact. It is then possible to measure the shear strength of a lubricant monolayer. The value obtained for calcium stearate is 250 g/mm^2. We are not yet certain whether this differs appreciably from the shear strength of the soap in bulk.

CONCLUSION

My main object here has been to give an outline of some of the more recent studies which our laboratory has been making on the friction of solids and to compare and contrast the behaviour of non-metallic solids with that of metals. Because of time limitation I have not dealt with lubricated solids, though this is an interesting field. The physical processes which occur during sliding are, of course, more complex than I have described here. In a more complete picture some account must be taken of the work of displacing the solid and of the combined stresses which operate during the shearing of the junctions. Also at appreciable sliding speeds the temperature at the points of contact will be high, and this will have a profound effect on their properties. A more complete account of the mechanism is given elsewhere.[1] In spite of this over simplification we have strong evidence that the mechanism of friction for non-metals is very similar to that for metals, since it is due primarily to adhesion at the points of local contact.

With certain solids the interfacial adhesion is low, and these give an abnormally low friction. P.T.F.E. is an example and also ice or krypton near their melting points. For most solids, however, whether they are plastic, brittle, or elastic, the surface adhesion can be very strong and the function μ due primarily to this. The difference in the behaviour of the various solids is due mainly to the difference in their mechanical properties, since it is this which determines both the area of true contact and the shear properties of the interfacial junction.

ACKNOWLEDGMENT

I wish to thank my colleagues, whose names are given in the text, for permission to quote unpublished work.

Reference

[1] Bowden, F. P., and Tabor, D. "The Friction and Lubrication of Solids," Oxford: Clarendon Press, revised reprint, 1954.

PRESENTATION OF THE REDWOOD MEDAL

The President: It is with very great pleasure that I welcome Dr Bowden to the ranks of Redwood Medallists. He is the tenth recipient of the Medal, which was introduced in 1921 in honour of the Founder-President of the Institute, but is the first non-member of the Institute to receive it. It is peculiarly fitting that this honour should be conferred on a distinguished scientist whose work has been concerned with the subject with which the late Sir Boverton Redwood was so closely identified. Sir Boverton's interests ranged over the whole field of petroleum science, but it is for his viscometer that his name is known to every student of petroleum technology.

DR F. P. BOWDEN

In 1869, at the age of twenty-three, he was appointed Secretary of the Petroleum Association, having decided to devote his main interest to mineral oil. Redwood's earliest work was in connexion with the flash point of mineral oils, on which he gave evidence before a Select Committee of the House of Lords in 1872. For the next ten years his work was very largely concerned with this problem, including the effect of barometric pressure on the evolution of volatile constituents of oil. These researches involved studies at high altitudes in the Alps and in pressure chambers in Berlin, to be followed, in 1882, by a visit to India to investigate the influence of climatic conditions on the testing of petroleum. In 1883 he visited most of the oil-producing localities of Europe and in 1886 of the U.S.A. and Canada. On his return he turned his attention to the viscosity of lubricating oils and designed the viscometer which, since that time, has been standard in petroleum-testing laboratories throughout the world.

In the late 'eighties, in co-operation with Sir Frederick Abel, Redwood investigated the cause of accidents with oil lamps and drafted regulations for their construction and use. In the early 'nineties, also in co-operation with Abel, he visited Egypt to report on the bulk transport of oil through the Suez Canal. This led, naturally, to his researches into the cause of explosions in vessels carrying oil cargoes, resulting in 1894 in the award by the Institution of Civil Engineers of the Telford Premium for his apparatus for detection of petroleum vapours. Then came the Redwood water-finder for determining the water level in oil storage tanks.

Redwood was one of the pioneers of the application of the internal combustion engine to road transport, and it is now fifty-five years since the first four-cylinder Daimler car was constructed to his order.

In 1904 he gave evidence before the Royal Commission on coal supplies and on the use of petroleum in ships and as a domestic fuel, later serving on Lord Fisher's Royal Commission on fuel and engines.

During the first world war he served on various government committees, and was appointed Director of Petroleum Research under the Ministry of Munitions.

He died in June 1919, and as the anonymous author of his obituary notice in the *Journal* of the Institute records, " He laboured in his vocation to the last. Even on the 2nd June, although already suffering from a chill that was destined to prove fatal within 48 hours, he telephoned to the Executive, by Lady Redwood's voice, a final message as to the sulphur content of the oil lately found in Derbyshire."

Many of the problems to which Redwood himself contributed have been the subject of addresses by former Redwood Medallists who have discussed: problems related to the origin and accumulation of oil; the application of geophysical methods to the search for oil; the production of petroleum; the chemistry of petroleum; the refining of petroleum; the electrification of the oilfields of Burma; the development of the internal combustion engine; and the last Medallist, education in the petroleum industry. But it has been left to Dr Bowden, the tenth recipient of the Medal, to deal with the subject of friction of solids, which is so closely related to Redwood's own work on the subject of viscometry.

The lecture which you have just heard from Dr Bowden will have left you with no doubt as to his qualifications for addressing you on this subject, but, for the record, it is customary for the President to enlarge on this theme.

A Tasmanian by birth, Dr Bowden graduated at the University of Tasmania in 1926. He then came to Cambridge, where he took his Ph.D. degree and was elected a Fellow of Gonville and Caius in 1929. He was appointed Humphrey Owen Jones Lecturer in Physical Chemistry in 1937 and Reader in Physical Chemistry in 1946. He received the Cambridge Sc.D. degree in 1934, and was elected a Fellow of the Royal Society in 1948. His researches are mainly on surface phenomena and range from the mechanism of electrodeposition to the initiation of explosions. During the war he was borrowed by the Australian Government and was in charge of the Tribophysics Division of the Commonwealth Scientific and Industrial Research Organization, Australia, from 1939 to 1945. Apart from numerous publications in scientific periodicals, he has published two books: " The Friction and Lubrica-

tion of Solids," 1950 (with D. Tabor), and "The Initiation and Growth of Explosion in Liquids and Solids," 1952 (with A. D. Yoffe). In addition to being Reader in Physical Chemistry, he is also Head of the Research Laboratory for the Physics and Chemistry of Surfaces, University of Cambridge.

Dr Bowden, it is my privilege and very great pleasure to present to you the Redwood Medal for your distinguished contributions to the science of lubrication, and to thank you for the erudite lecture to which we have listened with such interest.

Dr Bowden: I thank the President for the gracious and complimentary things he has said. In accepting this medal, which bears the name of its Founder-President, I would like to say only two things:

The first is my great appreciation of the honour which is done to me. I realize fully what a high and rare award it is, and I am very proud to join the distinguished ranks of the Redwood Medallists. My pleasure is all the greater because for me it came quite out of the "blue," since my past association with the Institute has been relatively slender.

Secondly, I would like the award to be regarded not as a recognition of my work only in this study of friction and lubrication but also as a joint award to my assistants and colleagues; in particular, I would mention Dr David Tabor. In fact, I think we should regard this handsome medal as an award to my laboratory.

A METHOD FOR APPROXIMATE DETERMINATION OF VISCOSITY–PRESSURE–TEMPERATURE RELATIONSHIPS FOR OILS*

RESULTS FROM AN INVESTIGATION OF COMPRESSIBILITY AND VISCOSITY

By SVEN LUNDBERG†

SUMMARY

This investigation was started in order to produce values of compressibility and viscosity especially for fuel oils, and thereby facilitate the work of designers of fuel injection equipment. A few other oils have been tested for the sake of completeness and the tests have covered pressures up to 1200 kg/cm² (about 17,000 p.s.i.) and temperatures between 20° and 125° C. The oils investigated were three light mineral fuel oils, two Swedish shale oils, one lubricating oil, and one vegetable oil.

For the determination of compressibility a compressibility meter has been used, designed by Gunst,[1] and the viscometer is of the ball-and-slanted-tube type.

Though comparatively few tests have been made, some interesting phenomena have appeared. The viscosity–pressure relationship at isothermal conditions appears to be linear in a half-logarithmic diagram, at least in the pressure-range from atmospheric pressure to 1200–1400 kg/cm² (20,000 p.s.i.), and for each oil the lines seem to come from one point which can be called the "viscosity–pressure pole." Viscosity values for four oils from a foreign investigation have been studied, too, and the same phenomena have appeared in this pressure-range.

On the basis of this phenomenon the author has given a method for approximate determination of the viscosity–pressure–temperature relationship for an oil, when the viscosity at atmospheric pressure is known at two temperatures and the viscosity under pressure is known at two temperatures, in which case the pressures have to correspond to the temperatures. Finally, a numerical example of the method is shown.

INTRODUCTION

THE investigation comprised determination of compressibility and viscosity for seven oils of different types. The maximum test pressure was 1200 kg/cm² (about 17,000 p.s.i.), and the temperature varied between 20° and 125° C.

In this paper, every tested oil has been given a number, as follows :

Oil No. 1. Light fuel oil (gas oil type) of good stability.
Oil No. 2. Light boiler fuel (Swedish shale oil).
Oil No. 3. Light boiler fuel (from Haifa).
Oil No. 4. Common automotive gas oil.
Oil No. 5. Lubricating oil, SAE 30.
Oil No. 6. Medium-heavy boiler fuel (Swedish shale oil).
Oil No. 7. Peanut oil, *Oleum arachidis* (only tested between 20° and 80° C).

Viscosity values for four other mineral oils have been obtained from a foreign investigation,[6] and these are :

A. California residual fuel, 700 SUS at 100° F
B. California residual fuel, 5000 SUS at 100° F
C. Nominal marine diesel fuel.
D. Light diesel fuel.

DETERMINATION OF COMPRESSIBILITY

Definition

The isothermal compressibility, here designated C is defined by Exline [13] as :

$$C = (1/P) \cdot (V_0 - V)/V_0 \text{ cm}^2/\text{kg}$$

where V is the volume in cm³ at the pressure P kg/cm², and V_0 volume in cm³ at atmospheric pressure.

Another definition is given in the same article [1] by Gunst :

$$C = -\frac{1}{V}\left(\frac{\delta V}{\delta P}\right)_T = -\frac{1}{V}\left(\frac{\delta \rho}{\delta P}\right)_T \left(\frac{\delta V}{\delta \rho}\right)_T = \frac{1}{\rho} \cdot \left(\frac{\delta \rho}{\delta P}\right)_T \text{ cm}^2/\text{kg}$$

P is the pressure in kg/cm², V the volume in cm³, and ρ the density in g/cm³. The subscript T means isothermal conditions.

For practical use the first definition seems to be the best, and is therefore used in this paper.

Description of Apparatus

The compressibility meter was made to the design of Gunst, of the Gulf Research and Development Co.

Fig 1 is a sectional diagram of the instrument. The test liquid is contained in a thin-walled brass bellows, whose spring constant and bulk compression are negligibly small. An application of pressure to the outside of the bellows compresses the test liquid within the bellows and results in a decrease in bellows length, which can be measured. The area of the bellows can be considered constant. A further description of the apparatus was made by Gunst.[1]

The required pressure was produced by a hand-pump and indicated on a manometer graduated from 0 to 1500 kg/cm². The pump was connected to the compressibility meter through a pipe of the same type as that used in small diesel engines, and the temperature

* MS received 19 October 1953.

† Chalmers University of Technology, Gothenburg, Sweden.

regulated by a thermostat. Ethylene glycol was used as the thermostat liquid. Fig 2 shows the compressibility meter and the thermostat.

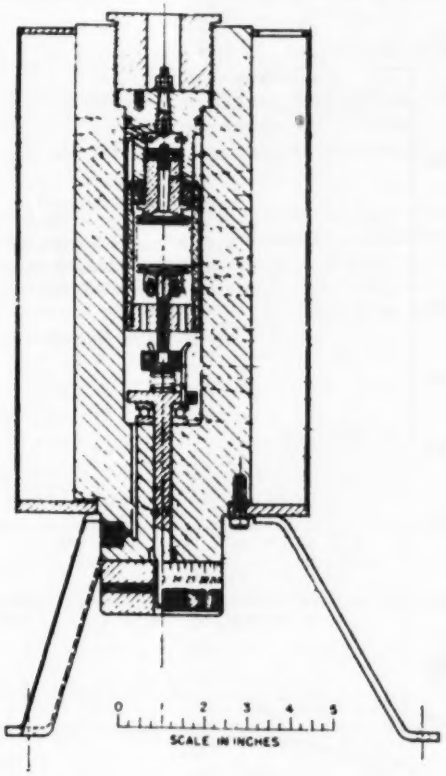

FIG 1
SECTIONAL DIAGRAM OF A COMPRESSIBILITY METER

Tests and Results

The test results of the density at atmospheric pressure are shown in Fig 3 as a function of the temperature. From the diagram the density–temperature relationship seems to be linear, so that if two values are known other values can be obtained from such a diagram.

If the density at 20° C is known the density at other temperatures t can be approximately obtained from the formula

$$\rho_{t,\,\mathrm{atm}} = \rho_{20^\circ,\,\mathrm{atm}} - k\,(t - 20)$$

where $\rho_{t,\,\mathrm{atm}}$ is the density in g/cm³ at the temperature t and atmospheric pressure and $\rho_{20^\circ,\,\mathrm{atm}}$ the density in g/cm³ at 20° C and atmospheric pressure. Values of the factor k, which have been obtained from Fig 3, are found in Table I.

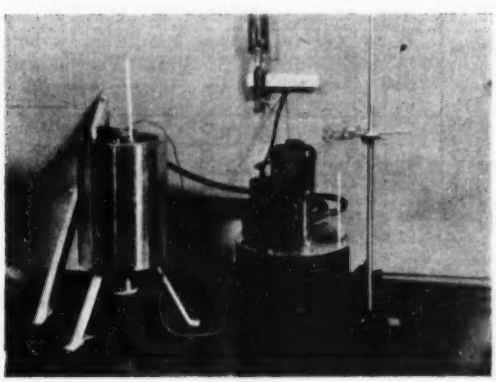

FIG 2
THE COMPRESSIBILITY METER AND THE THERMOSTAT
I

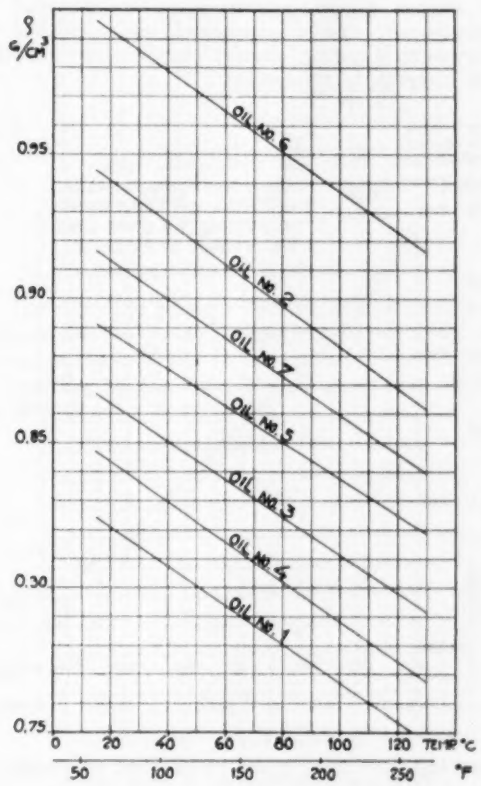

FIG 3
DENSITY–TEMPERATURE DIAGRAM FOR TESTED OILS

TABLE I

Oil type	Density g/cm³	The factor k
Mineral oil with the density in g/cm³ at 20° C	0·821	0·00068
	0·843	0·00068
	0·863	0·00065
	0·888	0·00063
Swedish shale oil	—	0·00071
Peanut oil	—	0·00067

For petroleum oils correct values, based on wider investigations, for the factor k can be obtained from the papers by Stott [10] and Beale.[11] Stott's values have been reduced to a nomograph,[12] which can be used for density corrections of mineral oils. Ubbelohde [9] gives some values for the factor k.

The compressibility was determined at temperatures from 20° to 125° C in intervals of 15° C. At every test temperature the pressure was varied from atmospheric to about 1200 kg/cm² (17,000 p.s.i.) in intervals of about 100 kg/cm² (1430 p.s.i.). The measurements were not taken until 30 seconds after the change in pressure to allow stabilization of pressure. At first the pressure was increased in intervals to maximum, then it was decreased with the same intervals to atmospheric.

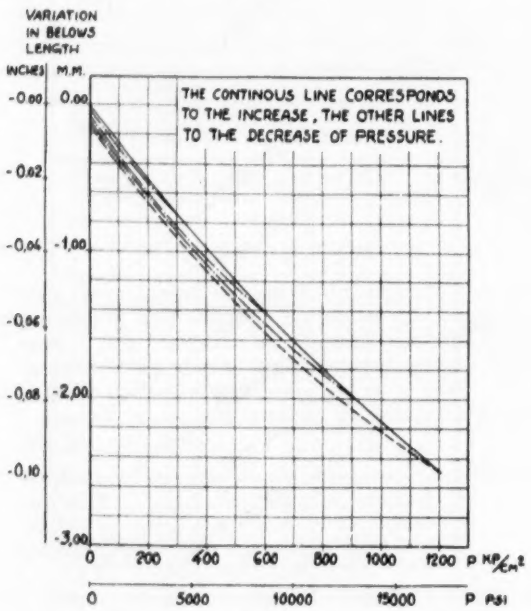
VARIATION IN BELOWS LENGTH
INCHES M.M.
THE CONTINOUS LINE CORRESPONDS TO THE INCREASE, THE OTHER LINES TO THE DECREASE OF PRESSURE.
P KP/CM²
P PSI

FIG 4

MEASURED VARIATIONS IN BELLOWS LENGTH AT DIFFERENT MAX PRESSURES, OIL NO. 1, TEMP 20° C

When the pressure was decreased an interesting phenomenon appeared. The bellows did not go back to the same length as before the compression, and further examination showed that the difference in length was larger the higher the maximum pressure had been. An example is shown in Fig 4. After a series of pressure loads as above, it took about a quarter of an hour before the bellows went back to the original length.

In another form of test the pressure was increased to 1200 kg/cm² and held constant for 0, 1, 5, and 10 minutes respectively, and then quickly decreased to atmospheric, the bellows length being determined every 30 seconds. Diagrams for oil Nos. 4 and 5 are shown in Figs 5 and 6. Similar diagrams are obtained for the other oils, and it can generally be said that the recovery time is longer, the greater the time of pressure load has been. As Figs 5 and 6 show, the curves of $1 - (\Delta V/V_0)$ do not have the same shape

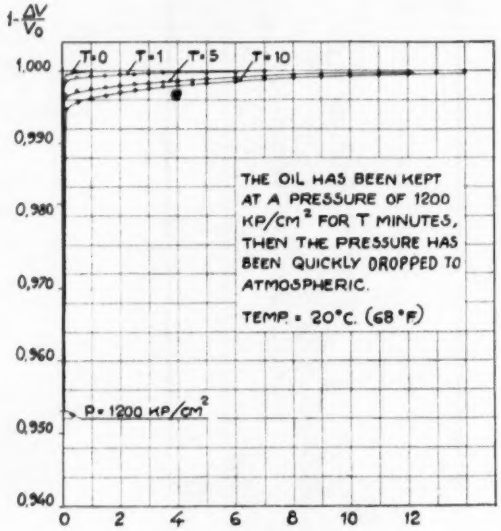
1-ΔV/V₀
T=0
T=1
T=5
T=10
THE OIL HAS BEEN KEPT AT A PRESSURE OF 1200 KP/CM² FOR T MINUTES, THEN THE PRESSURE HAS BEEN QUICKLY DROPPED TO ATMOSPHERIC.
TEMP. = 20°C. (68°F)
P = 1200 KP/CM²

FIG 5

PRINCIPAL DIAGRAM SHOWING THE REMAINING CHANGES IN VOLUME, OIL NO. 4

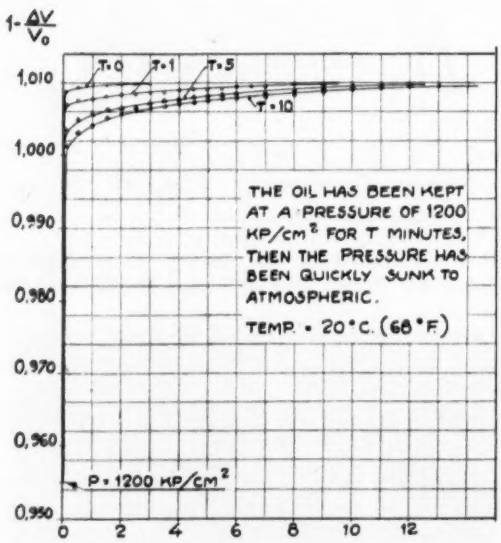
1-ΔV/V₀
T=0
T=1
T=5
T=10
THE OIL HAS BEEN KEPT AT A PRESSURE OF 1200 KP/CM² FOR T MINUTES, THEN THE PRESSURE HAS BEEN QUICKLY SUNK TO ATMOSPHERIC.
TEMP. = 20°C. (68°F)
P = 1200 KP/CM²

FIG 6

PRINCIPAL DIAGRAM SHOWING THE REMAINING CHANGES IN VOLUME, OIL NO. 5

for different oils, and so it can be supposed that the effects are manifestations of a property of the oil and not due to the apparatus. To clarify this point, further work is being carried out.

The density ρ at the pressure P and the temperature t can be easily obtained from

$$\rho \cdot V = \rho_0 \cdot V_0$$

$$\rho = \rho_0 \cdot V_0/V = \rho_0 \cdot V_0/(V_0 - \Delta V)$$
$$= \rho_0/[1 - (\Delta V/V_0)]$$

where V_0 = volume in cm³ at temperature t and atmospheric pressure;
ρ_0 = density in g/cm³ at temperature t and atmospheric pressure;
V = volume in cm³ at temperature t and pressure P.

Curves showing the test results of the density and compressibility under isothermal conditions as functions of the pressure have been drawn, and for oil No. 1 they are found in Figs 7 and 8 respectively. Fig 9 shows a combined compressibility diagram for all the tested oils at 20° and 125° C.

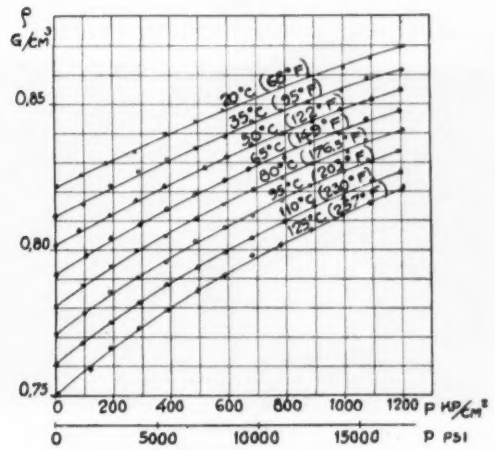

Fig 7

DENSITY–PRESSURE DIAGRAM, OIL NO. 1

For practical purposes it can be useful to know the relation between the volume V of a given quantity of oil at a certain temperature and pressure, and the volume V_{20} of the same quantity at 20° C and atmospheric pressure:

$$\rho \cdot V = \rho_{20} \cdot V_{20}$$
$$\therefore V/V_{20} = \rho_{20}/\rho$$

where ρ = density in g/cm³ at temperature t and pressure P;
ρ_{20} = density in g/cm³ at temperature 20° C and atmospheric pressure.

Test results of V/V_{20} at isothermal conditions have been drawn versus pressure, and Fig 10 shows this for oil No. 1. Combined diagrams for all the tested oils, one for each test temperature, have been drawn, and the V/V_{20} curves seem to pass through the same point at a fixed pressure, *e.g.* Fig 11 is such a diagram

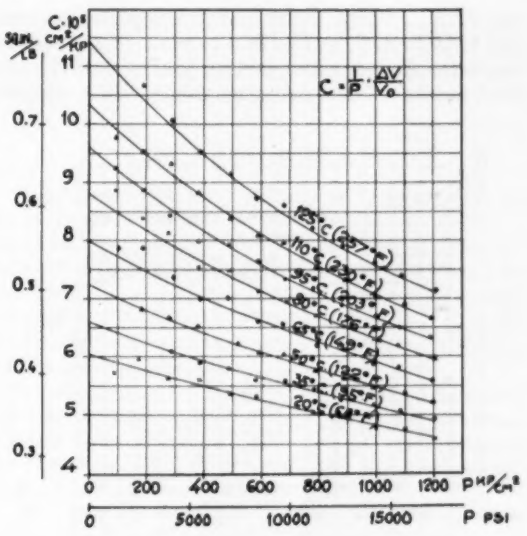

Fig 8

COMPRESSIBILITY C, OIL NO. 1

for 125° C. The relation between temperature and pressure for the points of intersection are found on the upper curve of Fig 21.

According to the equation $V/V_{20} = \rho_{20}/\rho$ above, the density ρ can be written as

$$\rho = (V_{20}/V) \cdot \rho_{20}$$

or

$$\rho = K \cdot \rho_{20 \text{ atm}},$$

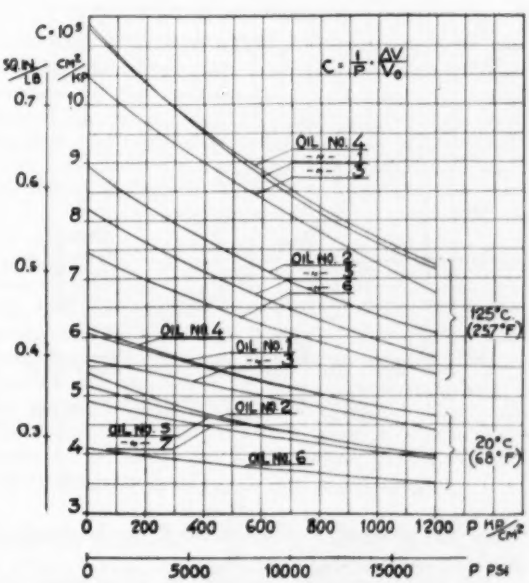

Fig 9

COMPRESSIBILITY C

where $\rho_{20\ atm}$ is the density at atmospheric pressure and 20° C and $K = (V_{20}/V)$. It must be noted that the factor K at one temperature has reference to one fixed pressure. Corresponding values of the temperature, the pressure, and the factor K can be obtained from the nomogram in Fig 21.

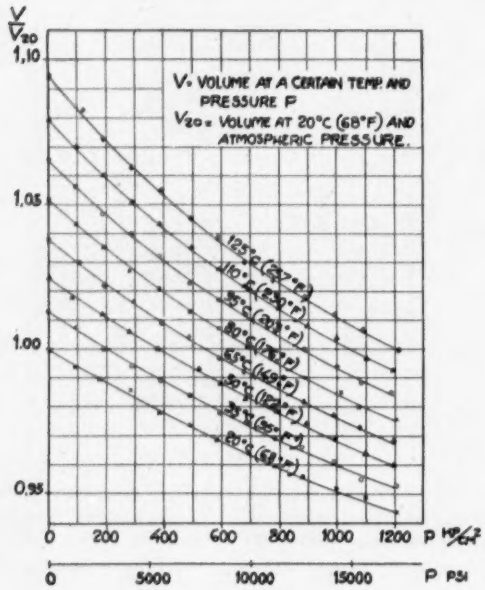
V/V20
1,10
1,05
1,00
0,95
V = VOLUME AT A CERTAIN TEMP AND PRESSURE P
V20 = VOLUME AT 20°C (68°F) AND ATMOSPHERIC PRESSURE.
0 200 400 600 800 1000 1200 P Kp/cm²
0 5000 10000 15000 P PSI

FIG 10

V/V20 AS A FUNCTION OF PRESSURE P, OIL NO. 1

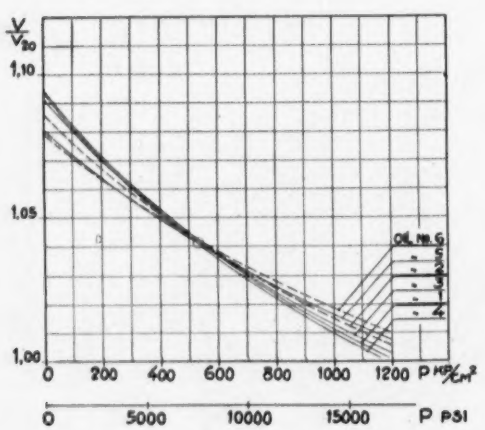

FIG 11

V/V20 AS A FUNCTION OF PRESSURE P, 125° C

This phenomenon finds application below (page 111) in the method for approximate determination of the viscosity of oils under pressure.

DETERMINATION OF VISCOSITY [2,3,4,5,7]

The rolling times in the viscometer give the absolute viscosity η in centipoises (cp). The kinematic viscosity υ in centistokes (cs) can be easily obtained if the density ρ in g/cm³ of the oil is known at the actual conditions

$$\upsilon = \eta/\rho$$

The unit centistokes is used throughout this report.

DESCRIPTION OF APPARATUS

The viscometer was designed after Hersey–Shore's project.[2] The apparatus consists of a thick-walled steel-tube (2—Fig 12), the inner diameter of which is 10·72 mm (0·422 inch). A $\frac{5}{16}$ inch dia steel ball rolls in this tube. The ends of the tube are closed by plugs (3) provided with electric contacts (6 and 13), which give electrical impulses when the ball passes

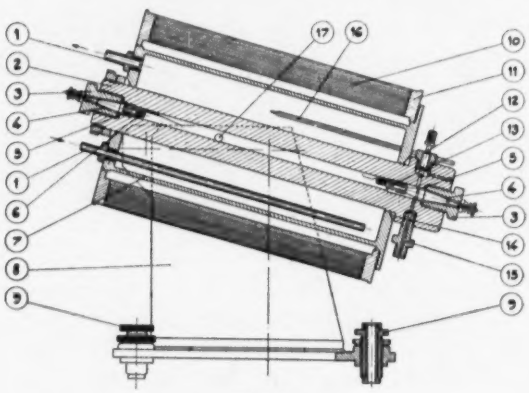

FIG 12

PRESSURE VISCOMETER

the beginning and the end of the roll distance. Conical nylon bushings (4) insulate the contacts from the rest of the plugs. Copper washers (5) are used as packings between the plugs and the tube. At one end of the tube there are an air outlet valve (12) and an inlet for pressure oil (15). Round the tube there is a jacket (7), in which the liquid from the thermostat circulates, passing in and out through hoses on the sockets (1). The jacket is set in a cradle (11), whose horizontal axle is carried by a stand (8). The cradle can incline the tube up to 60° in both directions. The inclination can be fixed by a pin that matches holes in a section as shown in Figs 13 and 15. The inclination of the tube can be 0°, 7·5°, 15°, 30°, 45°, and 60° in both directions. Two so-called 0-rings (14) are used as packings between the tube and the jacket. To reduce the heat radiation the cradle has an insulation (10), which consists of three layers of felt between two walls of brass sheet.

The temperature of the liquid around the tube can be read on the thermometer (16). The viscometer

is fixed to the table by three screws, and can be set exactly horizontally with three adjusting screws (9) on the bottom plate of the stand. The position is indicated by a circular spirit level.

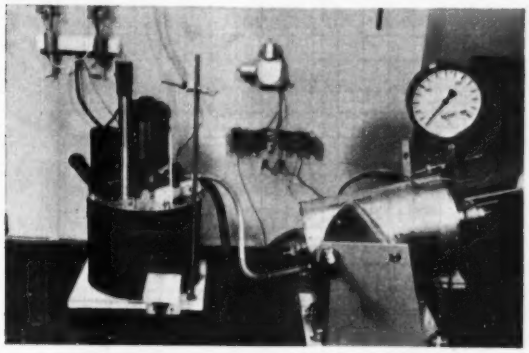

FIG 13

THE THERMOSTAT AND THE VISCOMETER FROM THE FRONT

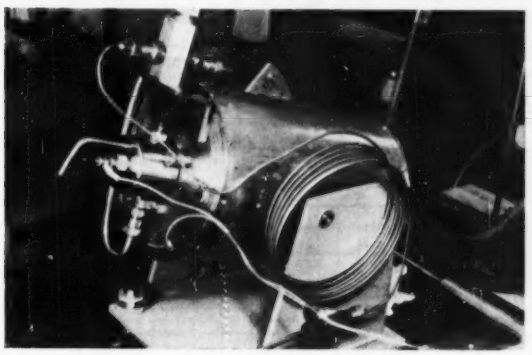

FIG 14

THE VISCOMETER FROM BEHIND

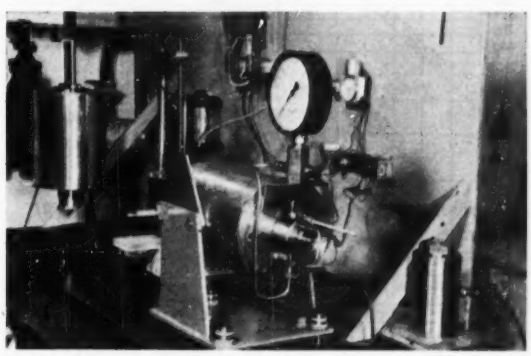

FIG 15

THE VISCOMETER FROM THE RIGHT SIDE

The pressure feed line has to permit a rocking motion of 120° round the horizontal axle of the cradle, and consists therefore of a pipe of 0·13 inch external and 0·04 inch internal diameter and about 13 feet in length, curved in a spiral as shown in Fig 14. To be independent of loss of pressure in this long and thin pipe a manometer has been placed after it on the viscometer (see Fig 13).

TESTS AND RESULTS

The roll times of the ball have been determined at an inclination of 15° on the viscometer tube at temperatures from 20° to 125° C in intervals of 15° C. At each temperature the pressure was increased in intervals of about 100 kg/cm² (1430 p.s.i.) from atmospheric pressure to about 1200 kg/cm² (17,000 p.s.i.), and then decreased again in the same intervals to atmospheric pressure.

It can be supposed that the phenomenon of hysteresis has an effect on the viscosity, but it has not been possible to establish any difference in the roll times for the heavy oils, because the roll times are much longer than the recovery times.

For light oils the roll times have been determined after a pressure load up to 1200 kg/cm² (17,000 p.s.i.) and a sudden decrease to atmospheric pressure, but in the following table a tendency to recovery is seen.

TABLE II

Oil No. 1 at 20° C

Time for the pressure load, minutes	Roll times in seconds with 15-second intervals of time							
0	1·71	1·70	1·70	1·69	1·68	1·68		
1	1·82	1·79	1·77	1·73	1·69	1·68		
5	1·82	1·81	1·76	—	1·70	1·70	1·69	1·68
10	1·85	—	1·80	1·73	1·73	1·71	1·71	1·70

For the calibration of the viscometer it is necessary to determine the viscosity at atmospheric pressure for the tested oils and a Hoeppler viscometer has been used for this purpose. In the pressure viscometer the absolute viscosity is supposed to be a function of the product of the roll time T and the driving power.[8]

$$\eta = \phi[T\ (\rho_0 - \rho)]$$

where η is the viscosity in cp, T the rolling time in seconds, and ρ_0 and ρ are the densities in g/cm³ of the ball and the liquid, respectively. The Hoeppler tests cover the range from 1 to 360 cp, and if the roll times from the pressure viscometer at atmospheric pressure are multiplied by $(\rho_0 - \rho)$ it is possible to dot in points on a diagram of η versus $T(\rho_0 - \rho)$. These points lie well together along a curve that seems to be linear for large values of T, and to satisfy the equation

$$\eta = T(\rho_0 - \rho)$$

where η is measured in cp, T in seconds, and ρ and ρ_0 in g/cm³. This diagram is expanded to a nomogram (Fig 16) in which the kinematic viscosity can be read in cs or Saybolt seconds directly from the roll time T seconds. Properly, the lines in the fourth quadrant

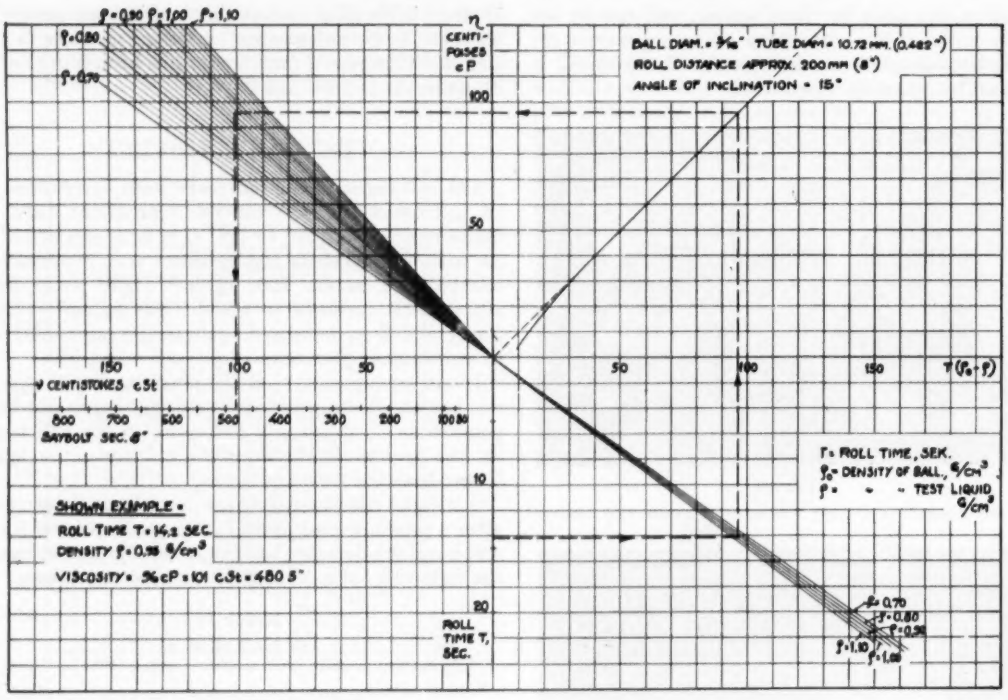
ρ = 0.90 ρ = 1.00 ρ = 1.10
ρ = 0.80
ρ = 0.70
η CENTI-POISES cP
BALL DIAM. = 5/16" TUBE DIAM = 10.72 mm (0.422")
ROLL DISTANCE APPROX. 200 mm (8")
ANGLE OF INCLINATION = 15°
ν CENTISTOKES c St
SAYBOLT SEC. U"
T = ROLL TIME, SEK.
ρ₀ = DENSITY OF BALL, g/cm³
ρ = " " TEST LIQUID g/cm³
SHOWN EXAMPLE:
ROLL TIME T = 14.2 SEC.
DENSITY ρ = 0.98 g/cm³
VISCOSITY = 5% cP = 101 c St = 480 S"
ROLL TIME T, SEC.
T (ρ₀ - ρ)

Fig 16

NOMOGRAM FOR DETERMINATION OF VISCOSITY

(Roll turns <20 sec)

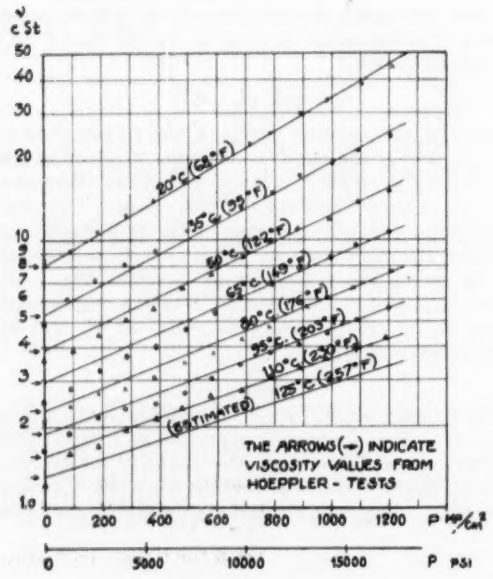

Fig 17

VISCOSITY–PRESSURE DIAGRAM, OIL NO. 1

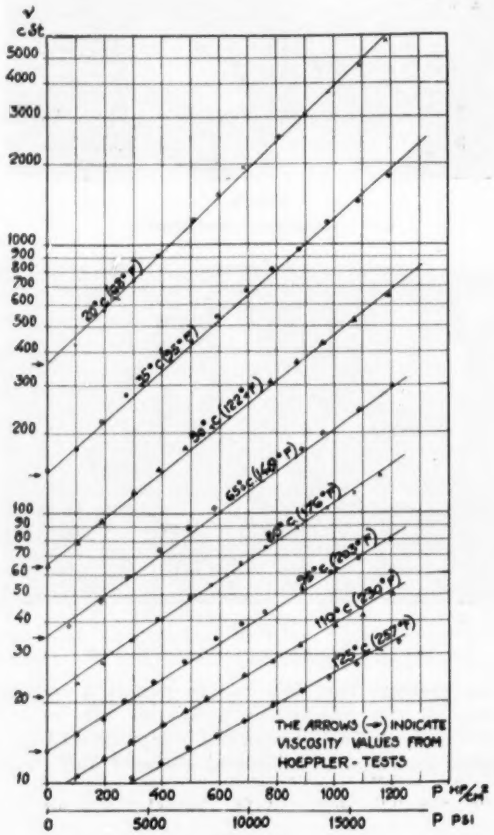
ν c St
20° C (68° F)
35° C (95° F)
50° C (122° F)
65° C (149° F)
80° C (176° F)
95° C (203° F)
110° C (230° F)
125° C (257° F)
THE ARROWS (→) INDICATE VISCOSITY VALUES FROM HOEPPLER - TESTS
P kp/cm²
P PSI

Fig 18

VISCOSITY–PRESSURE DIAGRAM, OIL NO. 5

should represent the values of $(\rho_0 - \rho)$, but as they lie so close together and the variation in ρ_0 is very small, the lines are calculated for $\rho_0 = 7{\cdot}770$ g/cm³, which is the value at a temperature of 50° C. For roll times T larger than 20 seconds, the equation above can be used to determine the absolute viscosity

When the lines are prolonged they all seem to come from the same point, as shown in Fig 19 for oil No. 1. For the other tested oils similar points are obtained.

For the foreign viscosity values [6] the same phenomena have appeared, at least in the pressure range

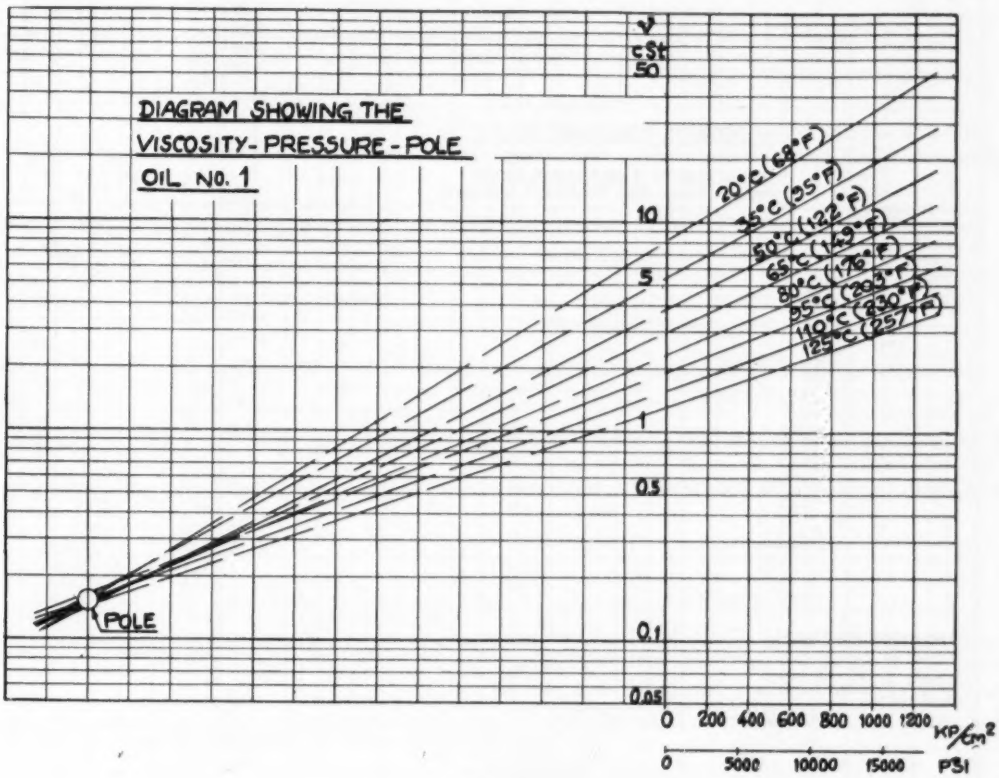

Fig 19

η in cp and then the kinematic viscosity ν in cs is obtained from the equation

$$\nu = \eta/\rho$$

with ρ in g/cm³.

When calculating the viscosity the density is obtained from density–pressure diagrams similar to that in Fig 7. The test results are dotted in on the diagrams with the pressure P on the horizontal axis and the logarithm of the viscosity log ν on the vertical axis, and in Figs 17 and 18 such diagrams for oil Nos. 1 and 5 are shown. The points seem to lie on straight lines for constant temperatures. For viscosities smaller than 2 cs, however, the points lie spread, and probably the apparatus is not very well adapted for such low viscosity values. Due to this, and the exactness of the Hoeppler tests, the lines have been laid through the latter values.

up to about 1400 kg/cm² (20,000 p.s.i.). For higher pressures the viscosity–pressure lines seem to bend slightly upwards.

The intersectional points for the viscosity lines have been called "viscosity–pressure poles" and shown dotted in on Fig 20 (cf. p. 104).

A METHOD FOR APPROXIMATE DETERMINATION OF THE VISCOSITY AT ANY TEMPERATURE AND PRESSURE UP TO 1400 KG/CM² (20,000 P.S.I.).

The test results give the idea of a method of approximate determination of the viscosity–pressure–temperature relationship for an oil when the viscosity at atmospheric pressure is known at two temperatures and the viscosity under pressure is known at two

temperatures, in which case the pressures must correspond to the temperatures.

For determination of the viscosity it is necessary to know the density at the actual temperature and pressure, so at first the density must be determined

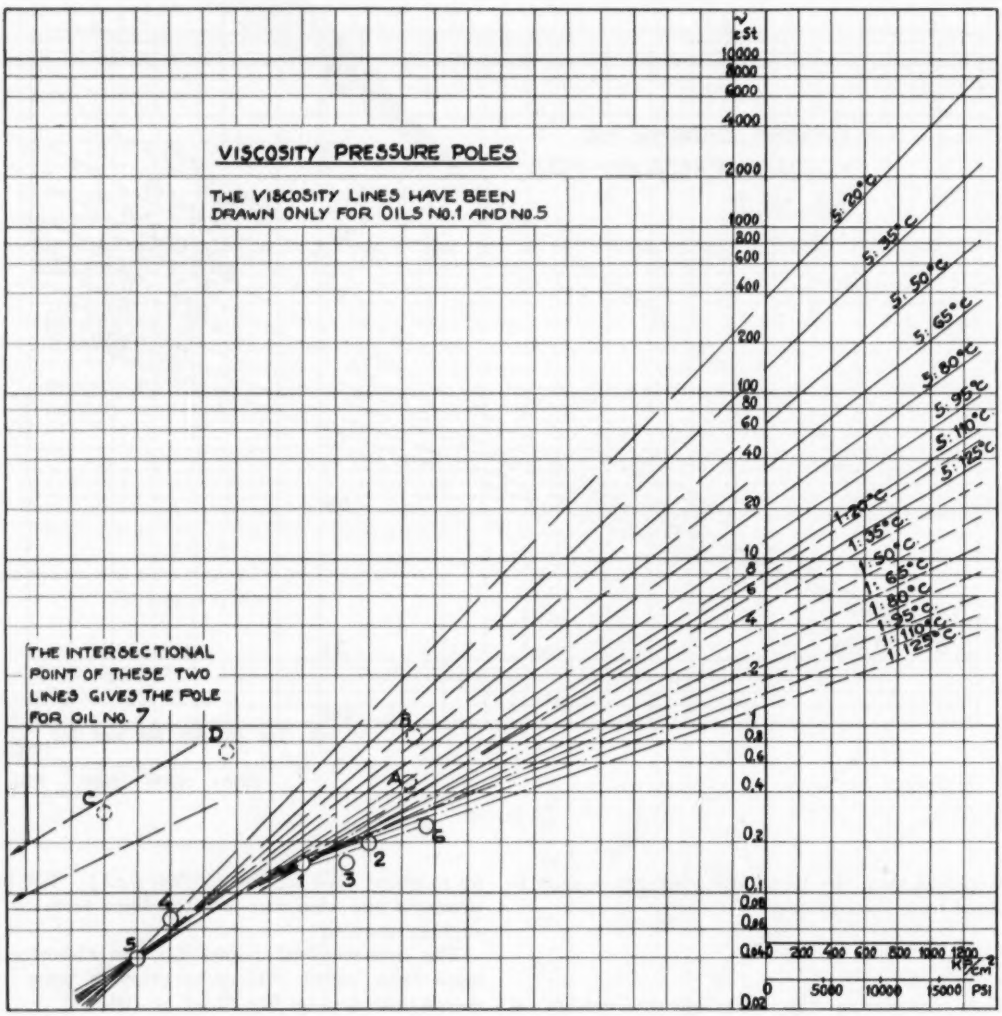

FIG 20

at 20° C ($\rho_{20°,\,atm}$) and one other temperature at atmospheric pressure either directly or by the method given above on pp. 105 and 106. Then the viscosity at atmospheric pressure can be determined at the above chosen temperatures, *e.g.* in a Hoeppler viscometer, and the values dotted in on Ubbelohde's viscosity–temperature diagram.[9] The viscosity at any temperature at atmospheric pressure can then be read in the diagram if a straight line is laid through the two points.

Approximate values of the density under pressure can be obtained with the aid of the nomogram in Fig 21. Two points (t_1, P_1) and (t_2, P_2) are chosen on the upper curve (the pressures must be higher than atmospheric), and then the corresponding values K_1 and K_2 can be read in the lower curve in the same nomogram. The densities are then obtained from

$$\rho_{t_1,\,P_1} = K_1 \cdot \rho_{20,\,atm}$$

and

$$\rho_{t_2,\,P_2} = K_2 \cdot \rho_{20,\,atm}.$$

Now the viscosity of the oil has to be determined at the temperature t_1 and the pressure P_1, and at the temperature t_2 and the pressure P_2.

Values of the viscosity at atmospheric pressure and

the temperatures t_1 and t_2 can be obtained from the viscosity–temperature diagram. These four values are dotted in on a diagram similar to Fig 19.

A straight line is laid through the two points corresponding to the temperature t_1 and another through the two points corresponding to t_2.

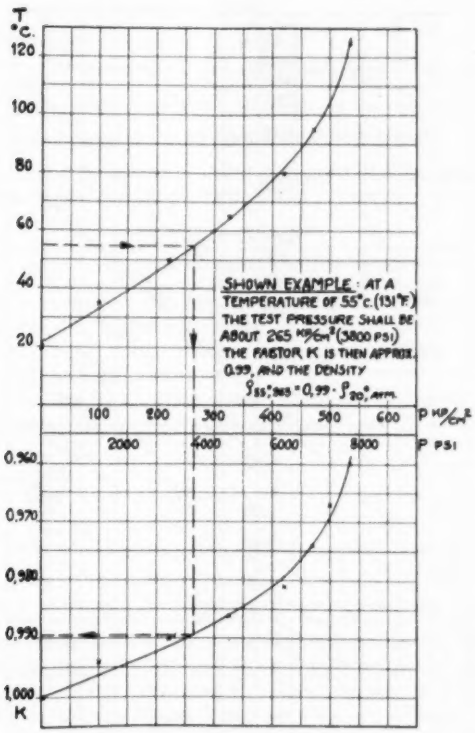

Fig 21

NOMOGRAM FOR DETERMINATION OF THE FACTOR K AND THE TEST PRESSURE

The intersection point of these lines is the viscosity–pressure pole. The diagram can be completed by laying lines through this pole and the points representing the viscosity values at atmospheric pressure, and the desired temperatures obtained from the viscosity–temperature diagram.

A diagram drawn in this way will have the same appearance as Fig 19. In such a diagram the viscosity at any temperature and any pressure actually used in fuel injection arrangements in diesel engines can be read.

To get a tolerably exact position of the viscosity–pressure pole, and of the viscosity lines in the diagram it is necessary to determine the viscosities with great accuracy.

If the values of the density are determined by compressibility tests as described above, the viscosity under pressure can be determined at two temperatures t_1 and t_2 and at any convenient pressure.

A numerical example has been carried out below to illustrate the method.

Example (Oil No. 5)

It is first necessary to determine the density at atmospheric pressure, 20° C, and one other temperature, *e.g.* 65° C. For oil No. 5 the values

$$\rho_{20°,\,atm} = 0{\cdot}888 \text{ g/cm}^3$$

and

$$\rho_{65°,\,atm} = 0{\cdot}860 \text{ g/cm}^3$$

are obtained.

If the density at 20° C is known and only approximate values are wanted the aforementioned formula can be used.

$$\rho_{t,\,atm} = \rho_{20°,\,atm} - k(t - 20)$$

With $\rho_{20°,\,atm} = 0{\cdot}888$ g/cm³ Table I gives

$$k = 0{\cdot}00063$$

The temperature $t = 65°$ C

$$\therefore \rho_{65°,\,atm} = 0{\cdot}888 - 0{\cdot}00063 \,.\, (65 - 20)$$

$$\therefore \rho_{65°,\,atm} = 0{\cdot}860 \text{ g/cm}^3$$

The viscosity at atmospheric pressure is then determined, *e.g.* in a Hoeppler viscometer at the same temperatures (20° C and 65° C respectively). The values

$$\nu_{20°,\,atm} = 362{\cdot}2 \text{ cs}$$

and

$$\nu_{65°,\,atm} = 34{\cdot}7 \text{ cs}$$

are obtained and dotted in on Ubbelohde's diagram (A and B in Fig 22). The points are connected with a line, and the viscosity at atm pressure is known at any temperature.

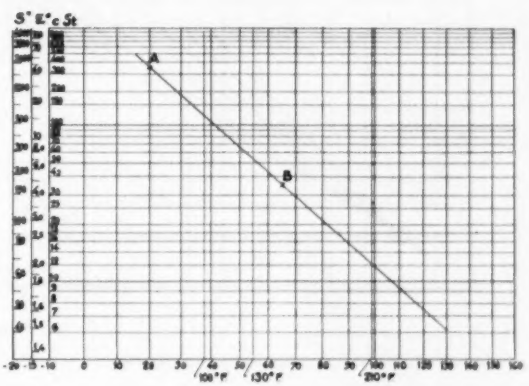

Fig 22

Then the viscosity under pressure is to be determined and the nomogram in Fig 21 used to get the test pressure and the density when the temperatures are fixed, *e.g.* to 50° C and 80° C.

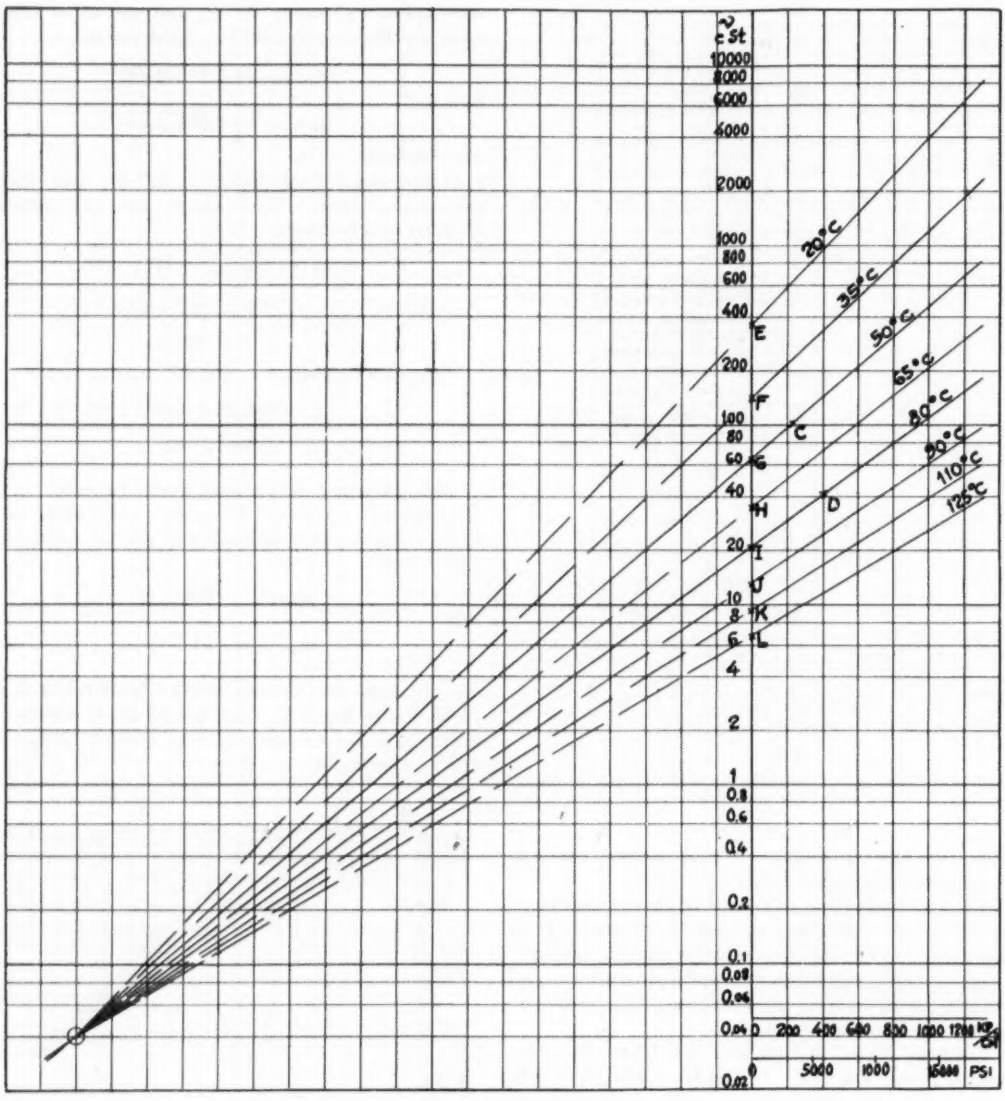
ν cSt
10000
8000
6000
4000
2000
1000
800
600
400
200
100
80
60
40
20
10
8
6
4
2
1
0.8
0.6
0.4
0.2
0.1
0.08
0.06
0.04
0.02
20°C
35°C
50°C
65°C
80°C
95°C
110°C
125°C
E
F
C
G
H
D
I
J
K
L
0 200 400 600 800 1000 1200 kp/cm²
0 5000 10000 15000 PSI

FIG 23

The temperature 50° C gives :

$$P = 230 \text{ kg/cm}^2 \text{ (3270 p.s.i.)}$$

$$K = 0{\cdot}991$$

$$\therefore \rho_{50°,230} = K \cdot \rho_{20°,atm} = 0{\cdot}991 \cdot 0{\cdot}888$$

$$= 0{\cdot}880 \text{ g/cm}^3$$

and the temperature 80° C gives :

$$P = 410 \text{ kg/cm}^2 \text{ (5830 p.s.i.)}$$

$$K = 0{\cdot}980$$

$$\therefore \rho_{80°,410} = 0{\cdot}980 \cdot 0{\cdot}888 = 0{\cdot}870 \text{ g/cm}^3$$

At these temperatures and pressures the following values of the viscosity are obtained :

$$\nu_{50°,230} = 101 \text{ cs}$$

$$\nu_{80°,410} = 41 \text{ cs}$$

On a diagram with the pressure on the horizontal axis and the logarithm of the viscosity in cs on the vertical axis, these values are dotted in (Fig 23, points C and D).

From Fig 22 the following values of the viscosity at atmospheric pressure are obtained :

ν = 360 cs	at the	temperature	20° C	(68° F)	(Point E)
ν = 140	,,	,,	35° C		(,, F)
ν = 66	,,	,,	50° C		(,, G)
ν = 35	,,	,,	65° C		(,, H)
ν = 20·9	,,	,,	80° C		(,, I)
ν = 13·4	,,	,,	95° C		(,, J)
ν = 9·3	,,	,,	110° C		(,, K)
ν = 6·7	,,	,,	125° C	(257° F)	(,, L)

These values are also dotted in on Fig 23 (the points E to L). Then there are two points for the temperature 50° C (C and G) and two points for the temperature 80° C (D and I). The intersection point of a line through C and G and another line through D and I gives the " pole," and then the lines for other temperatures can be drawn through the " pole " and the corresponding values of the viscosity at atmospheric pressure (the points E to L).

The viscosity for oil No. 5 can now be roughly read at temperatures and pressures actually used in fuel injection arrangements in diesel engines.

ACKNOWLEDGMENTS

The author wishes to express appreciation to AB Götaverken, Göteborg, and AB Svenska Shell, Stockholm, for their financial contribution and to C. O. Olsson, H. Robertsson, and J. Strömblad for carrying out the experimental work.

References

1. Gunst, S. B. *Trans. Amer. Soc. mech. Engrs*, 1950, **72**, 401.
2. Hersey, M. D., and Shore, H. *Mech. Engr*, 1928, **50**, 221.
3. Hersey, M. D., and Hopkins, R. F. *Mech. Engr*, 1945, **67**, 820.
4. Discussions. *Mech. Engr*, 1946, **68**, 576.
5. Dow, R. B., Fenske, M. R., and Morgan, H. E. *Industr. Engng Chem.*, 1937, **29**, 1078.
6. Habermann, C. E., Albright, R. E., and Killingsworth, R. B. " Residual Fuel Production and Utilization in Diesel Engines." Milan : Congrès International des Moteurs à Combustion Interne, 1953.
7. Schmidt, F. " The Technique of Heavy Oil Operation." Milan : Congrès International des Moteurs à Combustion Interne, 1953.
8. Höppler, F. *Z. für tech. Phys.*, 1933, **14**, 165.
9. Ubbelohde, L. " Zur Viskosimetrie." Leipzig : Verlag S. Hirzel, 1944.
10. Stott, V. *J. Inst. Petrol.*, 1940, **26**, 235.
11. Beale, E. S. L. *J. Inst. Petrol. Tech.*, 1937, **23**, 213.
12. Nissan, A. H. *Petrol. Refin.*, 1941, **20**, 408.
13. Exline, P. G. *Trans. Amer. Soc. mech. Engrs*, 1950, **72**, 401.

VISCOSITY AS A MEANS IN THE GRAPHICAL STATISTICAL ANALYSIS OF MINERAL OILS*

By C. BOELHOUWER and H. I. WATERMAN

PART I

SUMMARY

A structural group analysis of hydrogenated mineral oil fractions is described, allowing determination of the average number of rings per molecule (R_T), the percentage of carbon atoms present in ring structure (per cent C_R), the average molecular weight (M), and the density (d_4^{20}) from kinematic viscosity (centistokes at 20° C) and refractive index (n_D^{20}) data.

INTRODUCTION

In a recent publication [1] a method for the graphical statistical analysis of mineral oils was proposed. This was based on data of kinematic viscosity and refractive index (or density) of a large number of hydrogenated mineral oil fractions of different origins. These data allowed determination of the average number of rings per molecule (R_T) in good agreement with the results of the well known method of analysis, based on specific refraction $\left(\frac{n^2-1}{n^2+2}\cdot\frac{1}{d}\right)$ and molecular weight (the so-called "ring-analysis" [2]).

In this paper the method is extended to a determination of the percentage of carbon atoms in ring structure (per cent C_R) and compared with the results of the n–d–M method.[3] An approximate calculation of the molecular weight from kinematic viscosity and refractive index is described also.

Experimental Part. The physical data of the saturated mineral oil fractions, used in this paper, were already collected.[1]

The kinematic viscosity of the fractions was determined at 20° C with the aid of Ostwald type viscometers. When the oils were solid at 20° C the measurements were carried out at 40°, 60°, and 80° C; and the viscosity at 20° C determined by graphical extrapolation.

In Fig 1 the kinematic viscosities of the oils are plotted against their refractive index. This figure is exactly the same as that published,[1] it having been extended only by another set of curves representing per cent C_R, the percentage of carbon atoms in ring structure (assuming six-membered and kata-condensed rings [3]). The several sets of lines of Fig 1 allow a direct reading of the density (d_4^{20}), the average number of rings per molecule (R_T) and the percentage of carbon atoms in ring structure (per cent C_R) of saturated natural mineral oil fractions of known kinematic viscosity and refractive index.

On account of the legibility of the graph in Fig 1 no curves of equal molecular weight have been drawn. It is possible, however, from R_T and per cent C_R, to calculate the average molecular weight M of the fractions, M being given by the formulæ:

$$M = \frac{2800}{\%\,C_R}\cdot 3\,R_T \text{ when } R_T < 1$$

and $$M = \frac{2800}{\%\,C_R}\cdot (2\,R_T + 1) \text{ when } R_T > 1.$$

(compare [4]).

The results of these readings and calculations are collected in Table I and compared with the outcomes of the n–d–M-analyses [3] of the fractions.

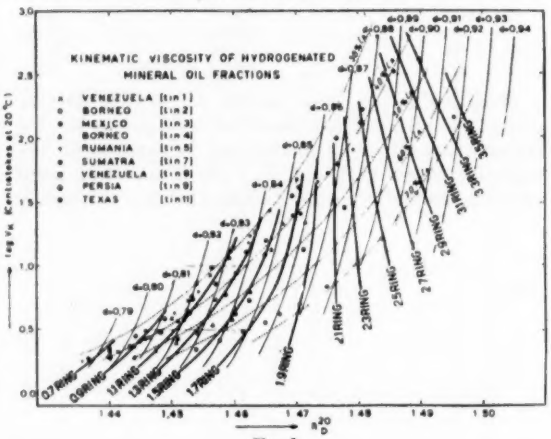

FIG 1

It can be concluded that viscosity measurements of saturated mineral oil fractions are of great importance for their structural analysis. Combined with refractive index determinations they allow a rapid and accurate characterization of these products.

References

[1] Boelhouwer, C., van Steenis, J., and Waterman, H. I. *Fuel, Lond.*, 1954, **33**, 60.

[2] Vlugter, J. C., Waterman, H. I., and van Westen, H. A. *J. Inst. Petrol. Tech.*, 1932, **18**, 735; 1935, **21**, 661; 1939, **25**, 678; *Chem. Weekbl.*, 1932, **29**, 226; and Leendertse, J. J., Vlugter, J. C., Waterman, H. I., and van Westen, H. A. *Chem. Weekbl.*, 1942, **39**, 282, 299.

[3] van Nes, K., and van Westen, H. A. "Aspects of the Constitution of Mineral Oils," Amsterdam: 1951.

[4] *Ibid.*, p. 258.

* MS received 17 August 1953.

TABLE I

Physical Constants of Saturated Mineral Oil Fractions

Oil fractions		n_D^{20}	d_4^{20}	V_K centistokes 20° C	Mol Weight	n-d-M-analysis		Estimated from n_D^{20} and V_K (Fig 1)			Mol weight (calculated)
						% C_R	R_T	d_4^{20}	% C_R	R_T	
Venezuela (tin 1)	fraction 1	1·4411	0·7990	2·11	166	43	0·9	0·798	40	0·8	170
	2	1·4462	0·8080	2·75	185	42	1·0	0·808	40	0·9	190
	3	1·4499	0·8154	3·84	201	42	1·1	0·814	37	1·0	230
	4	1·4525	0·8197	5·30	235	36	1·1	0·819	34	1·0	250
	5	1·4560	0·8260	8·30	247	37	1·2	0·825	32	1·1	280
	6	1·4592	0·8320	11·4	275	36	1·3	0·832	32	1·1	280
	7	1·4626	0·8390	17·3	304	34	1·4	0·838	31	1·3	320
	8	1·4657	0·8453	27·0	344	33	1·6	0·844	30	1·4	350
	9	1·4702°	0·8546°	47·2°	381	34	1·8	0·853	32	1·7	390
	10	1·4831°	0·8815°	630°	599	34	3·2	0·880	33	3·0	590
Borneo (tin 2)	fraction 1	1·4536	0·8325	2·18	174	62	1·5	0·832	62	1·4	170
	2	1·4576	0·8406	2·56	181	63	1·6	0·840	63	1·6	190
	3	1·4614	0·8482	3·02	184	64	1·7	0·848	65	1·7	190
	4	1·4649	0·8554	3·57	186	67	1·8	0·857	66	1·8	190
	5	1·4673	0·8605	4·15	192	67	1·8	0·861	67	1·8	190
	6	1·4705	0·8673	4·98	195	69	1·9	0·868	68	1·9	200
	8	1·4748	0·8756	7·06	216	67	2·1	0·877	69	2·0	200
	9	1·4799	0·8872	10·4	226	70	2·4	0·888	70	2·3	220
	10	1·4837	0·8945	16·2	238	70	2·5	0·895	70	2·5	240
	11	1·4894	0·9070	37·1	266	70	2·9	0·906	70	2·8	260
	12	1·4956	0·9199	147	310	70	3·4	0·917	67	3·4	330
	13	1·5077°	0·9444°	4790	560	72	4·3	—	—	—	—
Mexico (tin 3)	fraction 1	1·4396	0·7944	1·95°	179	54	0·8	0·795	40	0·8	170
	2	1·4447	0·8049	2·53°	198	36	0·9	0·805	40	0·9	190
	3	1·4518	0·8198	3·75°	221	40	1·1	0·820	42	1·1	210
	4	1·4585	0·8337	5·82°	239	45	1·4	0·834	44	1·3	230
	5	1·4649	0·8471	12·1°	263	44	1·6	0·846	43	1·5	260
	6	1·4707	0·8593	25·5°	301	44	1·9	0·857	42	1·8	310
	7	1·4766	0·8717	62·5°	342	45	2·3	0·869	41	2·1	350
	8	1·4808	0·8801	129°	395	44	2·6	0·877	40	2·5	420
Borneo (tin 4)	fraction 1	1·4438	0·8067	1·92	164	51	1·0	0·807	50	1·0	170
	2	1·4472	0·8140	2·15	168	54	1·2	0·814	52	1·1	170
	3	1·4506	0·8210	2·48	173	57	1·2	0·822	54	1·2	180
	4	1·4540	0·8282	2·95	178	57	1·3	0·829	54	1·3	190
	5	1·4564	0·8331	3·40	186	56	1·4	0·834	54	1·4	200
	6	1·4596	0·8392	3·76	189	57	1·5	0·841	58	1·5	190
	7	1·4601	0·8404	4·18	197	56	1·5	0·842	56	1·5	200
	9	1·4621	0·8429	6·25	217	51	1·5	0·844	52	1·5	220
	11	1·4660°	0·8480°	13·3°	279	42	1·6	0·848	43	1·5	260
	12	1·4714°	0·8598°	22·0°	310	42	1·9	0·860	45	1·8	290
	13	1·4765°	0·8681°	45·2°	356	41	2·1	0·869	44	2·1	330
	residue	1·4885°	0·8960°	417°	464	46	3·4	0·898	44	3·2	470
Rumania (tin 5)	fraction 1	1·4354	0·7857	1·79	164	34	0·7	0·786	55	0·6	140
	2	1·4405	0·7963	2·54	175	37	0·8	0·794	51	0·7	190
	3	1·4456	0·8064	3·09	199	36	0·9	0·806	35	0·9	220
	4	1·4503	0·8153	4·26	219	37	1·0	0·815	36	1·0	230
	5	1·4542	0·8220	6·26	240	36	1·1	0·822	34	1·0	250
	6	1·4580	0·8299	9·75	277	35	1·2	0·829	32	1·1	280
	7	1·4623	0·8389	15·1	300	35	1·4	0·838	33	1·3	310
	8	1·4678°	0·8493°	21·6°	343	34	1·7	0·851	38	1·6	310
	9	1·4731°	0·8611°	45·7°	380	36	2·0	0·862	38	1·9	350
	10	1·4792°	0·8736°	81·3°	420	39	2·4	0·874	42	2·4	390
Sumatra (tin 6)	fraction 1	1·4369	0·7918	—	170	38	0·8	—	—	—	—
	2	1·4382	0·7944	1·77	179	37	0·8	0·793	40	0·8	170
	3	1·4414	0·8010	1·87	176	42	0·9	0·802	46	0·9	160
	4	1·4447	0·8077	2·35	179	45	1·0	0·807	43	0·9	180
	5	1·4475	0·8137	2·47	185	48	1·1	0·814	48	1·1	190
	6	1·4504	0·8195	3·08	193	49	1·2	0·819	47	1·1	190
	7	1·4535	0·8260	3·38	200	51	1·3	0·826	50	1·3	200
	8	1·4564	0·8318	4·34	209	49	1·4	0·832	48	1·3	210
	9	1·4591	0·8375	5·39	219	49	1·5	0·837	48	1·4	220
	10	1·4624	0·8439	7·16	227	50	1·6	0·844	49	1·5	230
	11	1·4658	0·8507	10·1	251	48	1·7	0·850	48	1·6	250
	12	1·4703	0·8605	15·9	269	49	1·9	0·859	49	1·8	260
	13	1·4773	0·8753	34·0	292	52	2·3	0·874	50	2·2	300
Sumatra (tin 7)	fraction 1	1·4366	0·7889	1·80	169	35	0·7	0·789	36	0·7	160
	2	1·4399	0·7953	2·11	175	37	0·8	0·795	37	0·8	180
	3	1·4432	0·8021	2·34	188	37	0·9	0·802	40	0·9	190
	4	1·4456	0·8068	2·69	196	37	0·9	0·807	40	0·9	190
	5	1·4480	0·8121	3·05	202	40	1·0	0·812	40	1·0	210
	6	1·4509	0·8179	3·66	215	40	1·1	0·818	41	1·1	220
	7	1·4523	0·8200	4·45	224	39	1·1	0·820	38	1·1	240
	8	1·4532	0·8208	5·68	243	35	1·1	0·820	34	1·0	250
	9	1·4539	0·8215	7·25	263	32	1·0	0·820	30	1·0	280
	10	1·4563	0·8251	9·6	291	29	1·1	0·824	29	1·0	290
	11	1·4593°	0·8312°	12·7°	321	30	1·2	0·831	29	1·1	310
	12	1·4634°	0·8381°	18·4°	353	30	1·3	0·839	32	1·3	320
	13	1·4694°	0·8505°	35·5°	380	31	1·7	0·852	34	1·6	350
	residue	1·4857°	0·8870°	330°	475	41	3·0	0·888	41	3·0	480
Venezuela (tin 8)	fraction 1	1·4508	0·8204	2·68	176	55	1·2	0·823	52	1·2	180
	2	1·4624	0·8440	5·31	205	55	1·5	0·846	54	1·6	220
	3	1·4712	0·8635	13·4	255	53	2·0	0·862	53	1·8	240
	4	1·4778	0·8750	28·6	303	50	2·3	0·876	53	2·2	290
Persia (tin 9)	fraction 1	1·4364	0·7873	1·88	170	32	0·7	0·787	34	0·7	170
	2	1·4398	0·7940	2·27	186	31	0·8	0·793	34	0·7	170
	3	1·4441	0·8027	2·82	193	35	0·9	0·802	35	0·8	190
	4	1·4488	0·8123	3·85	213	36	1·0	0·812	35	0·9	220
	5	1·4532	0·8213	5·46	225	39	1·1	0·821	36	1·0	240
	6	1·4570	0·8288	7·22	245	40	1·3	0·829	37	1·1	240
	7	1·4619	0·8390	12·8	274	39	1·5	0·838	36	1·3	280
	9	1·4704°	0·8567°	41·7°	340	38	1·9	0·854	34	1·7	360
	10	1·4765°	0·8692°	100°	377	40	2·2	0·867	36	2·2	420
	11	1·4827°	0·8784°	170°	426	41	2·6	0·877	38	2·5	440
Texas (tin 11)	fraction 1	1·4399	0·7963	1·92	165	42	0·9	0·797	41	0·8	160
	2	1·4438	0·8041	2·35	180	41	0·9	0·804	41	0·9	180
	3	1·4481	0·8125	3·09	192	43	1·0	0·813	41	1·0	200
	4	1·4527	0·8217	4·24	212	44	1·2	0·822	40	1·1	220
	5	1·4569	0·8297	5·36	225	45	1·3	0·831	43	1·3	230
	6	1·4603	0·8362	8·73	260	40	1·4	0·836	39	1·3	260
	7	1·4651	0·8462	15·6	294	39	1·6	0·845	38	1·5	290
	8	1·4695°	0·8553°	24·6°	330	39	1·8	0·854	39	1·7	320
	9	1·4750°	0·8663°	53·0°	367	40	2·2	0·866	39	2·0	360
	10	1·4802°	0·8774°	132°	415	41	2·6	0·876	39	2·5	430

° extrapolated

PART II

SUMMARY

A structural group analysis of mineral oil fractions is described, based on the determination of kinematic viscosity, refractive index, and density of the fractions. The method allows estimation of carbon distribution, aromatic and naphthenic ring content, and average molecular weight of olefin-free mineral oil fractions boiling above the gasoline range.

INTRODUCTION

In a recent publication [1] on the applicability of viscosity data for the graphical statistical analysis of mineral oil, diagrams were developed which showed the relation between the kinematic viscosity and the chemical composition of hydrogenated mineral oil fractions. The diagrams also depicted a characterization of aromatic-free natural petroleum fractions of known kinematic viscosity and refractive index which were in good agreement with the ring-analysis method [2] and the *n–d–M* method.[3]

To extend the applicability of the method to aromatic oils the same line of thought was followed as that adopted by former investigators.[4] This involves consideration of theoretical hydrogenated oils, the physical constants of which have to be calculated from those of the original oils by means of "prediction factors." In this paper formulæ are given which predict, from kinematic viscosity (centistokes at 20° C), refractive index (n_D^{20}), and density (d_4^{20}) of natural mineral oil fractions, the corresponding constants of (theoretical) completely hydrogenated oils (derived from the natural oil fractions in question). This allows graphical determination of M, the molecular weight, per cent C_R, the total percentage of carbon

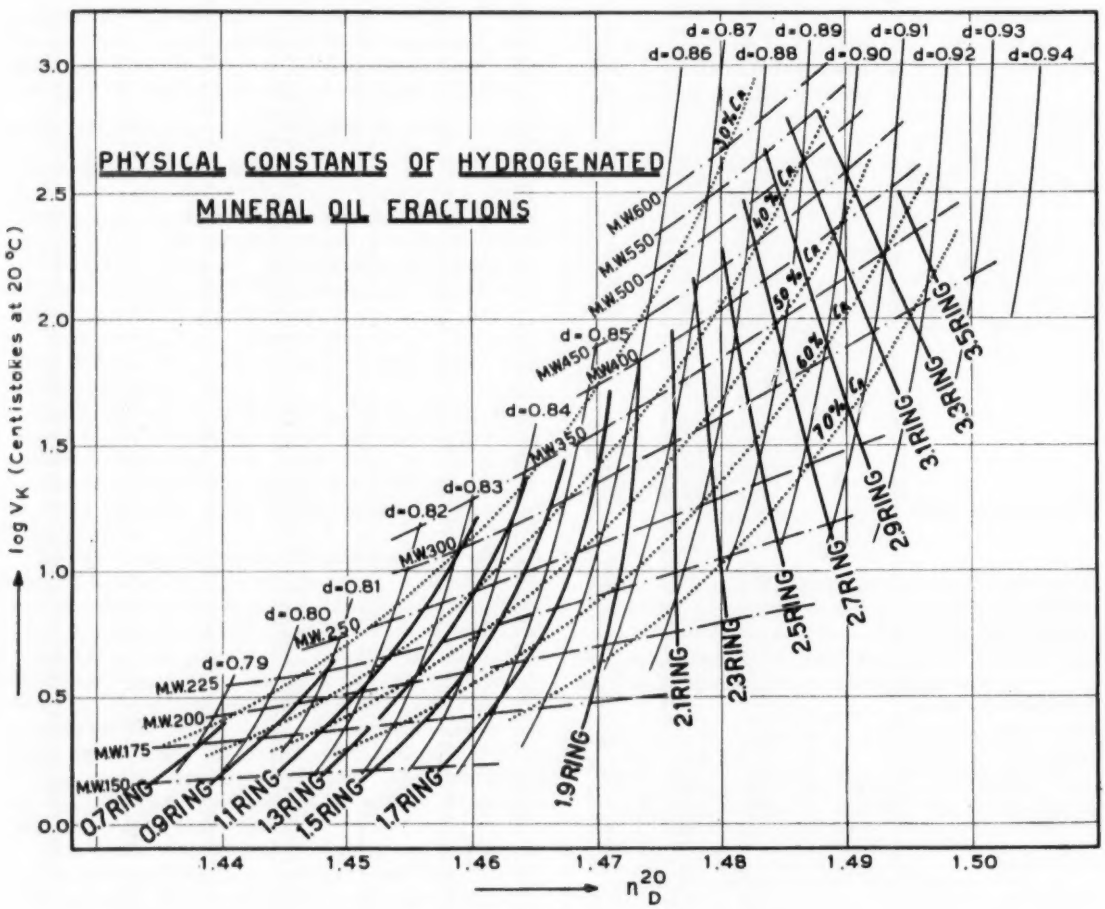

Fig 1

atoms present in aromatic and naphthenic ring structure, and R_T, the total number of rings per molecule. The aromatic content, calculated as per cent C_A, the percentage of carbon atoms in aromatic ring structure, follows from the difference between the densities of the original and corresponding (theoretical) hydrogenated fractions. For sulphur-containing oils a sulphur correction can be applied.

DESCRIPTION OF V_k–n–d METHOD

(1) The method is based on determination of kinematic viscosity V_k (centistokes at 20° C), refractive index n (n_D^{20}), and density d (d_4^{20}) of natural mineral oil fractions. In the case of sulphur-containing oils determination of the sulphur content allows application of a sulphur correction in the analysis. It can be expected that this correction is applicable only for relatively low sulphur contents.

(2) The method is executed graphically. A graph is used (Fig 1) showing the relation between viscosity, refractive index, density, and molecular weight of saturated mineral oil fractions. From this graph a density d' can be read, using refractive index and kinematic viscosity of the oil under examination. In general, there will be a difference Δd between this graphically observed value d' and the real density d of the oil sample.

(3) From Δd the density d^* of the (theoretical) completely hydrogenated oil can be calculated with a good approximation according to the formula :

$$d^* = d - 0{\cdot}62\ \Delta d - 0{\cdot}008\%\ \mathrm{S}$$

The kinematic viscosity V_k^* of the completely hydrogenated oil may be given with an accuracy, sufficient for the analysis, by the following approximate relation:

$$\log V_k^* = (1 - 3\Delta d) \log V_k + \Delta d$$

(4) With the aid of d^* and $\log V_k^*$ it is possible to read from Fig 1 the molecular weight M, the percentage of carbon atoms in ring structure per cent C_R, and the average total number of rings per molecule R_T of the hydrogenated sample corresponding with the oil under examination. These values are the same for the original oil fraction (assuming that the molecular weight does not alter on hydrogenation).

(5) The aromatic content, expressed as per cent C_A, the percentage of carbon atoms in aromatic structure, can be estimated directly from Δd :

$$\%\ C_A = 600\Delta d - (40\Delta d)^2$$

no sulphur correction being necessary. The average number of aromatic rings per molecule, R_A, follows from the equations :

$$2R_A + 1 = \frac{M \times \%\ \mathrm{C}_A}{2800}, \text{ when } R_A > 1$$

or

$$3R_A = \frac{M \times \%\ \mathrm{C}_A}{2800}, \text{ when } R_A < 1.$$

(6) Finally, the percentages of carbon atoms in naphthenic and paraffinic structure (% C_N and % C_P, respectively) and the average number of naphthenic rings per molecule R_N, are given by the equations :

$$\%\ \mathrm{C}_N = \%\ \mathrm{C}_R - \%\ \mathrm{C}_A$$
$$R_N = R_T - R_A$$
$$\%\ \mathrm{C}_P = 100 - \%\ C_R$$

DISCUSSION

In Table I the results of the V_k–n–d analysis of approx 100 natural mineral oil fractions of different origin are compared with those of the n–d–M method. It can be concluded that the agreement of both the methods is very good. Thus it is possible, in the analysis of mineral oil fractions, to replace the rather laborious molecular weight determinations by kinematic viscosity measurements.

According to the data of Table I the method is applicable for mineral oil fractions with a molecular weight of approx 160 to 600 ;[1] for higher molecular oils, especially when the aromatic content is rather high, the applicability is often restricted by the boundaries of the graph.

Very likely the method can be extended easily to oils containing less than 30 per cent C_R, or less than 0·7 rings per molecule. The construction of the sets of curves in Fig 1 was limited by the composition of the oils available for investigation.[1]

The development and check of the V_k–n–d method is based mainly on compairsons with the results of the n–d–M method and the ring analysis of our fractions. No direct data, based on ultimate analyses and molecular weight determinations of oils before and after their hydrogenation, were available. It may be necessary, therefore, to improve and refine the graph and the formulæ, given above, when more accurate data become available.

ACKNOWLEDGMENTS

Thanks are due to J. Cornelissen, R. Notenboom, and J. van Rooy for executing the viscosity measurements.

References

[1] Boelhouver, C., van Steenis, J., and Waterman, H. I. *Fuel Lond.*, 1954, **33**, 60.

[2] Vlugter, J. C., Waterman, H. I., and van Westen, H. A. *J. Inst. Petrol. Tech.*, 1932, **18**, 735; 1935, **21**, 661; 1939, **25**, 678. Leendertse, J. J., Vlugter, J. C., Waterman, H. I., and van Westen, H. A. *Chem. Weekbl.*, 1942, **39**, 282, 299.

[3] van Nes, K., and van Westen, H. A. "Aspects of the Constitution of Mineral Oils," Amsterdam : 1951.

[4] Vlugter, J. C., Waterman, H. I., and van Westen, H. A. *J. Inst. Petrol. Tech.*, 1935, **21**, 661; Leendertse, J. J., *ibid* p. 314.

TABLE I

Physical Properties of Natural Mineral Oil Fractions

Oil fractions	n_D^{20} (n)	d_4^{20} (d)	% S	log V_k on 20° C.	d' from n and V_k (Fig. 1)	$\Delta d = (d' - d)$	$d^* = d - 0{\cdot}62\,\Delta d - 0{\cdot}008\%\,S$	log $V_k^* = (1 - 3\,\Delta d)\log V_k + \Delta d$	V_k–n–d analysis: Determined from F_d^* and log V_k^* in Fig. 1: Mol weight	% C_N	R_T	V_k–n–d analysis: Calculated: % $C_A = 600\,\Delta d - (40\,\Delta d)^2$	R_A	% C_N	R_N	% C_P	n–d–M analysis: Mol weight (experim.)	% C_N	R_T	% C_A	R_A	% C_N	R_N	% C_P
Tin 1, Venezuela																								
Fraction 1	1·4551	0·8158	0·07	0·350	0·836	0·0202	0·8027	0·35	175	43	0·9	11	0·2	32	0·7	57	164	46	0·9	12	0·3	34	0·6	54
2	1·4595	0·8235	0·11	0·439	0·845	0·0215	0·8099	0·43	190	42	1·0	12	0·3	30	0·7	58	181	44	1·0	13	0·3	31	0·7	56
3	1·4638	0·8307	0·2 †	0·609	0·852	0·0213	0·8160	0·59	215	38	1·0	12	0·3	26	0·7	62	203	40	1·0	13	0·3	27	0·7	60
4	1·4673	0·8363	0·33	0·735	0·859	0·0227	0·8196	0·71	235	36	1·0	13	0·4	23	0·6	64	224	37	1·0	13	0·4	24	0·6	63
5	1·4708	0·8429	0·41	0·949	0·864	0·0211	0·8265	0·91	270	33	1·1	12	0·4	21	0·7	67	261	35	1·1	12	0·4	23	0·7	65
6	1·4746	0·8510	0·56	1·126	0·872	0·0210	0·8335	1·08	290	33	1·2	12	0·4	21	0·8	67	277	35	1·2	13	0·4	22	0·8	65
7	1·4794	0·8594	0·63	1·33	0·882	0·0226	0·8404	1·26	320	33	1·3	13	0·5	20	0·8	67	303	34	1·3	13	0·5	21	0·8	66
8	1·4836	0·8675	0·77	1·54	0·891	0·0235	0·8473	1·46	345	33	1·5	13	0·5	20	1·0	67	339	33	1·5	13	0·5	20	1·0	67
9	1·4890*	0·8778*	0·86	1·78 *	0·903	0·0252	0·8553	1·68	375	34	1·7	14	0·6	20	1·1	66	381	34	1·9	13	0·6	21	1·3	66
Tin 2, Borneo																								
Fraction 1	1·4617	0·8414	—	0·344	0·853	0·0116	0·8342	0·34	170	63	1·5	7	0·1	56	1·4	37	176	61	1·5	5	0·1	56	1·4	39
2	1·4687	0·8530	—	0·382	0·871	0·0180	0·8418	0·38	170	65	1·6	10	0·2	55	1·4	35	177	64	1·6	9	0·2	55	1·4	36
3	1·4761	0·8657	—	0·500	0·888	0·0223	0·8519	0·49	180	66	1·7	12	0·3	54	1·4	34	180	67	1·7	12	0·3	55	1·4	33
4	1·4835	0·8762	—	0·535	0·907	0·0308	0·8571	0·52	185	68	1·8	17	0·4	51	1·4	32	184	67	1·8	17	0·4	50	1·4	33
5	1·4909	0·8868	—	0·644	0·924	0·0372	0·8637	0·61	190	68	1·8	20	0·5	48	1·3	32	190	68	1·8	21	0·5	47	1·3	32
6	1·4989	0·8978	—	0·736	0·944	0·0462	0·8692	0·68	195	69	1·9	24	0·6	45	1·3	31	198	67	1·9	24	0·6	43	1·3	33
7	1·5070	0·9100	—	0·838	0·964	0·0540	0·8765	0·76	205	70	2·0	28	0·7	42	1·3	30	209	67	2·1	27	0·7	40	1·4	33
8	1·5146	0·9186	—	0·941	0·983	0·0644	0·8736	0·82	210	70	2·1	32	0·8	38	1·3	30	214	66	2·1	31	0·8	35	1·3	34
Tin 3, Mexico																								
Fraction 1	1·4488	0·8058	0·17	0·290	0·820	0·0142	0·7956	0·29	170	40	0·8	8	0·2	32	0·6	60	176	37	0·8	7	0·2	30	0·6	63
2	1·4559	0·8187	0·28	0·412	0·836	0·0173	0·8058	0·41	190	40	0·9	10	0·2	30	0·7	60	194	38	0·9	8	0·2	30	0·7	62
3	1·4656	0·8363	0·45	0·605	0·857	0·0207	0·8201	0·59	215	41	1·1	12	0·3	29	0·8	59	213	42	1·1	11	0·3	31	0·8	58
4	1·4759	0·8551	0·72	0·850	0·880	0·0249	0·8339	0·81	235	42	1·3	14	0·4	28	0·9	58	243	42	1·3	14	0·4	28	0·9	58
5	1·4850	0·8723	1·00	1·12 *	0·901	0·0287	0·8465	1·05	260	44	1·5	16	0·5	28	1·0	56	269	43	1·5	15	0·5	28	1·0	57
6	1·4950	0·8906	1·25	1·52 *	0·922	0·0314	0·8611	1·41	300	44	1·8	17	0·6	27	1·2	56	308	43	1·8	16	0·6	27	1·2	57
7	1·5033	0·9055	1·50	1·94 *	0·940	0·0345	0·8721	1·77	350	43	2·2	19	0·8	24	1·4	57	355	43	2·1	17	0·8	26	1·3	57
8	1·5106	0·9183	1·62	2·35 *	0·957	0·0387	0·8813	2·12	400	43	2·6	21	1·0	22	1·6	57	396	43	2·5	19	0·9	24	1·6	57
Tin 4, Borneo																								
Fraction 1	1·4707	0·8363	—	0·230	0·881	0·0447	0·8086	0·24	160	54	1·0	24	0·5	30	0·5	46	152	56	1·1	26	0·5	30	0·6	44
2	1·4759	0·8446	—	0·297	0·893	0·0484	0·8146	0·30	165	54	1·1	25	0·5	29	0·6	46	159	56	1·1	27	0·5	29	0·6	44
3	1·4818	0·8537	—	0·350	0·907	0·0533	0·8206	0·35	170	55	1·2	28	0·6	27	0·6	45	166	57	1·2	28	0·6	29	0·6	43
4	1·4884	0·8634	—	0·428	0·923	0·0596	0·8264	0·41	180	56	1·3	30	0·6	26	0·7	44	169	59	1·3	31	0·6	28	0·7	41
5	1·4935	0·8709	—	0·480	0·935	0·0641	0·8317	0·45	185	57	1·4	32	0·7	25	0·7	43	175	60	1·3	32	0·7	28	0·6	40
6	1·4968	0·8766	—	0·548	0·942	0·0654	0·8360	0·51	190	58	1·4	33	0·7	25	0·7	42	181	56	1·4	33	0·7	23	0·7	44
7	1·4994	0·8804	—	0·634	0·948	0·0676	0·8384	0·57	195	56	1·5	33	0·8	23	0·7	44	188	55	1·4	33	0·8	22	0·6	45
9	1·4981	0·8808	—	0·83	0·940	0·0592	0·8441	0·74	220	53	1·5	30	0·8	23	0·7	47	216	50	1·5	29	0·8	21	0·7	50
11	1·4970*	0·8808*	—	1·15 *	0·933	0·0522	0·8484	1·03	250	46	1·6	27	0·8	19	0·8	54	272	41	1·6	25	0·8	16	0·8	59
12	1·5046*	0·8946*	—	1·47 *	0·949	0·0544	0·8609	1·27	280	47	1·8	28	0·9	19	0·9	53	313	41	1·8	25	1·0	16	0·8	59
Tin 5, Rumania																								
Fraction 1	1·4483	0·8029	—	0·250	0·820	0·0171	0·7923	0·26	165	40	0·7	10	0·2	30	0·5	60	158	41	0·8	11	0·2	30	0·6	59
2	1·4539	0·8123	—	0·356	0·832	0·0197	0·8001	0·36	180	39	0·8	11	0·2	28	0·6	61	172	41	0·9	12	0·2	29	0·7	59
4	1·4662	0·8328	—	0·619	0·858	0·0252	0·8172	0·60	215	38	1·0	14	0·4	24	0·6	62	208	39	1·0	15	0·4	24	0·6	61
5	1·4695	0·8390	—	0·823	0·863	0·0240	0·8241	0·79	245	36	1·1	13	0·4	23	0·7	64	232	37	1·1	15	0·4	22	0·7	63
6	1·4733	0·8469	—	1·03	0·870	0·0231	0·8326	0·99	275	35	1·2	13	0·4	22	0·8	65	264	37	1·2	14	0·4	23	0·8	63
7	1·4795	0·8580	0·17	1·23 *	0·884	0·7260	0·8419	1·16	290	37	1·4	14	0·5	23	0·9	63	291	36	1·4	14	0·5	22	0·9	64
8	1·4858*	0·8694*	0·2 †	1·45 *	0·898	0·0286	0·8516	1·35	310	39	1·6	16	0·6	23	1·0	61	339	34	1·6	15	0·6	19	1·0	66
10	1·5003*	0·8958*	0·25	2·03 *	0·932	0·0362	0·8714	1·85	370	41	2·3	20	0·8	21	1·5	59	390	39	2·2	17	0·8	22	1·4	61

Tin 6, Sumatra																								
Fraction 1	1·4510	0·8090	—	0·152	0·831	0·0220	0·7954	0·16	150	50	0·8	12	0·2	38	0·6	50	159	45	0·9	11	0·2	34	0·7	55
2	1·4530	0·8125	—	0·228	0·834	0·0215	0·7992	0·24	160	48	0·9	12	0·2	36	0·7	52	155	48	0·9	12	0·2	36	0·7	52
3	1·4558	0·8178	—	0·243	0·841	0·0232	0·8034	0·25	160	49	0·9	13	0·2	36	0·7	51	165	47	1·0	12	0·2	35	0·8	53
4	1·4591	0·8238	—	0·332	0·847	0·0232	0·8094	0·33	170	48	1·0	13	0·3	35	0·7	52	171	48	1·0	13	0·3	35	0·7	52
5	1·4632	0·8302	—	0·413	0·855	0·0248	0·8148	0·41	180	49	1·1	14	0·3	35	0·8	51	176	49	1·1	15	0·3	34	0·8	51
6	1·4670	0·8372	—	0·439	0·865	0·0278	0·8200	0·43	185	51	1·2	15	0·4	36	0·8	49	187	50	1·2	15	0·4	35	0·8	50
7	1·4713	0·8444	—	0·520	0·874	0·0296	0·8260	0·50	200	51	1·3	17	0·4	34	0·9	49	193	51	1·2	17	0·4	34	0·8	49
8	1·4759	0·8519	—	0·606	0·885	0·0331	0·8314	0·58	205	51	1·3	18	0·4	33	0·9	49	200	53	1·3	19	0·5	34	0·8	47
9	1·4800	0·8586	0·05	0·735	0·893	0·0344	0·8369	0·69	215	50	1·4	19	0·5	31	0·9	50	209	50	1·4	20	0·5	30	0·9	50
10	1·4835	0·8651	—	0·866	0·900	0·0349	0·8435	0·81	230	50	1·5	19	0·5	31	1·0	50	222	49	1·5	20	0·5	29	1·0	51
11	1·4878	0·8726	—	1·03	0·910	0·0374	0·8494	0·95	240	49	1·6	20	0·6	29	1·0	51	243	47	1·6	20	0·6	27	1·0	53
12	1·4951	0·8857	—	1·25	0·926	0·0403	0·8607	1·13	255	51	1·8	22	0·7	29	1·1	49	266	48	1·8	21	0·7	27	1·1	52
13	1·5078	0·9065	0·33	1·68	0·955	0·0485	0·8738	1·48	290	51	2·2	25	0·9	26	1·3	49	306	48	2·2	24	0·9	24	1·3	52
Tin 7, Sumatra																								
Fraction 1	1·4539	0·8081	—	0·220	0·837	0·0289	0·7902	0·23	160	40	0·7	16	0·3	24	0·4	60	165	36	0·8	15	0·3	21	0·5	64
2	1·4571	0·8136	—	0·277	0·843	0·0294	0·7954	0·28	170	40	0·8	16	0·3	24	0·5	60	173	36	0·8	16	0·3	20	0·5	64
3	1·4619	0·8213	—	0·340	0·854	0·0327	0·8010	0·34	175	41	0·9	18	0·4	23	0·5	59	181	37	0·8	18	0·4	19	0·4	63
4	1·4662	0·8284	—	0·415	0·863	0·0346	0·8069	0·41	185	40	0·9	19	0·4	21	0·5	60	188	38	0·9	20	0·5	18	0·4	62
5	1·4702	0·8351	—	0·487	0·872	0·0369	0·8122	0·47	195	41	1·0	20	0·5	21	0·5	59	194	39	1·0	21	0·5	18	0·5	61
6	1·4731	0·8401	—	0·562	0·878	0·0379	0·8166	0·54	205	40	1·0	21	0·5	19	0·5	60	209	38	1·0	20	0·5	18	0·5	62
7	1·4732	0·8409	—	0·648	0·877	0·0361	0·8185	0·62	220	38	1·0	20	0·5	18	0·5	62	213	38	1·0	20	0·5	18	0·5	62
8	1·4717	0·8392	—	0·751	0·871	0·0318	0·8195	0·71	235	36	1·0	17	0·5	19	0·5	64	237	33	1·0	17	0·5	16	0·5	67
9	1·4703	0·8380	—	0·869	0·865	0·0270	0·8212	0·83	255	32	1·0	15	0·5	17	0·5	68	260	29	1·0	15	0·5	14	0·5	71
10	1·4707	0·8396	—	1·013	0·863	0·0234	0·8251	0·97	285	30	1·0	13	0·4	17	0·6	70	280	28	1·0	13	0·5	15	0·5	72
11	1·4728*	0·8439*	—	1·14*	0·867	0·0231	0·8296	1·08	300	30	1·1	13	0·5	17	0·6	70	318	27	1·1	12	0·5	15	0·6	73
12	1·4754*	0·8496*	—	1·37*	0·871	0·0214	0·8363	1·30	340	28	1·2	12	0·5	16	0·7	72	340	29	1·2	12	0·5	17	0·7	71
13	1·4820*	0·8628*	—	1·59*	0·886	0·0232	0·8484	1·50	350	32	1·5	13	0·6	19	0·9	68	375	30	1·6	12	0·6	18	1·0	70
Tin 8, Venezuela																								
Fraction 1	1·4654	0·8400	0·3	0·418	0·861	0·0210	0·8246	0·41	180	56	1·3	12	0·2	44	1·1	44	175	59	1·3	12	0·3	47	1·0	41
2	1·4852	0·8755	0·85	0·785	0·906	0·0305	0·8498	0·74	215	57	1·6	17	0·4	40	1·2	43	205	57	1·6	18	0·5	39	1·1	43
3	1·5013	0·9036	1·25	1·29	0·942	0·0384	0·8698	1·18	250	56	2·0	21	0·6	35	1·4	44	248	56	2·0	21	0·6	35	1·4	44
4	1·5143	0·9255	1·7	1·95	0·970	0·0445	0·8843	1·74	320	52	2·5	24	0·9	28	1·6	48	304	53	2·3	22	0·8	31	1·5	47
Tin 9, Persia																								
Fraction 1	1·4460	0·7982	0·15	0·258	0·814	0·0158	0·7872	0·26	165	36	0·7	9	0·2	27	0·5	64	162	35	0·7	9	0·2	26	0·5	65
2	1·4510	0·8077	0·19	0·337	0·825	0·0173	0·7955	0·34	180	37	0·8	10	0·2	27	0·6	63	174	36	0·8	10	0·2	26	0·6	64
3	1·4573	0·8188	0·32	0·458	0·838	0·0192	0·8043	0·45	195	37	0·9	11	0·3	26	0·6	63	186	38	0·9	12	0·3	26	0·6	62
4	1·4640	0·8305	0·48	0·590	0·853	0·0225	0·8128	0·57	215	37	1·0	13	0·3	24	0·7	63	201	39	0·9	14	0·3	25	0·6	61
5	1·4701	0·0819	0·69	0·748	0·866	0·0241	0·8214	0·72	235	37	1·1	14	0·4	23	0·7	63	220	41	1·0	15	0·4	26	0·6	59
6	1·4768	0·8538	0·96	0·916	0·882	0·0282	0·8286	0·87	250	36	1·1	16	0·5	20	0·6	64	242	39	1·2	16	0·5	23	0·7	61
7	1·4847	0·8679	1·22	1·16	0·898	0·0301	0·8394	1·08	280	38	1·3	17	0·6	21	0·7	62	273	38	1·3	17	0·6	21	0·7	62
8	1·4923	0·8814	1·35	1·44	0·915	0·0336	0·8498	1·33	310	38	1·6	18	0·7	20	0·9	62	300	39	1·5	18	0·7	21	0·8	61
9	1·4979*	0·8914*	1·50	1·76*	0·927	0·0356	0·8573	1·60	350	37	1·8	19	0·8	18	1·0	63	342	37	1·7	18	0·8	19	0·9	63
10	1·5067*	0·9066*	1·51	2·08*	0·949	0·0424	0·8682	1·85	380	38	2·1	23	1·1	15	1·0	62	387	38	2·1	20	1·0	18	1·1	62
11	1·5148*	0·9196*	1·73	2·42*	0·968	0·0484	0·8758	2·15	420	39	2·5	25	1·2	14	1·3	61	434	38	2·3	22	1·2	16	1·1	62
Tin 11, Texas																								
Fraction 1	1·4510	0·8082	0·04	0·253	0·827	0·0188	0·7962	0·26	165	43	0·8	11	0·2	32	0·6	57	164	41	0·9	11	0·2	30	0·7	59
2	1·4564	0·8174	0·04	0·352	0·839	0·0216	0·8037	0·35	175	42	0·9	12	0·3	30	0·6	58	176	41	0·9	12	0·3	29	0·6	59
3	1·4630	0·8283	0·06	0·467	0·853	0·0247	0·8125	0·46	190	43	1·0	14	0·3	29	0·7	57	187	43	1·0	15	0·3	28	0·7	57
4	1·4688	0·8379	0·10	0·622	0·865	0·0271	0·8203	0·60	215	41	1·1	15	0·4	26	0·7	59	201	44	1·1	17	0·4	27	0·7	56
5	1·4735	0·8465	0·19	0·728	0·876	0·0295	0·8267	0·69	225	42	1·2	16	0·4	26	0·8	58	220	44	1·2	17	0·5	27	0·7	56
6	1·4780	0·8552	0·24	0·992	0·883	0·0278	0·8361	0·94	255	40	1·3	16	0·5	24	0·8	60	246	41	1·3	16	0·5	25	0·8	59
7	1·4841	0·8665	0·20	1·25	0·896	0·0295	0·8466	1·17	285	40	1·5	16	0·5	24	1·0	60	276	40	1·5	16	0·6	24	0·9	60
8	1·4895*	0·8764*	0·32	1·45*	0·908	0·0316	0·8542	1·34	300	41	1·7	17	0·6	24	1·1	59	304	40	1·7	17	0·6	23	1·1	60
9	1·4952*	0·8872*	0·29	1·78*	0·920	0·0328	0·8646	1·64	340	41	2·0	18	0·8	23	1·2	59	345	39	2·0	17	0·7	22	1·3	61
10	1·5022*	0·8997*	0·39	2·24*	0·935	0·0353	0·8747	2·04	405	40	2·4	19	1·0	21	1·4	60	401	40	2·3	18	0·9	22	1·4	60

* Extrapolated. † Estimated.

COMPARISON OF VISCOSITIES OF AMERICAN GRADES OF CUTBACK BITUMENS DETERMINED BY SAYBOLT FUROL VISCOMETER AND STANDARD TAR VISCOMETER *

By C. M. GOUGH †

THE viscosity ranges of American grades of cutback bitumen are specified by means of the Saybolt Furol viscometer. American cutbacks are used in many parts of the world where viscosities are measured by the British Standard tar viscometer. Confusion frequently arises on account of these two methods, and there is a continual demand for a means of converting from one system of measurement to the other.

Accordingly, viscosity determinations, using both instruments to obtain a direct comparison, were made at the Road Research Laboratory on cutback bitumens prepared from three different petroleum crudes, including one of high wax content, corresponding to the R.C. and M.C. 1, 2, 3, 4, and 5 grades. Samples corresponding to the lower, intermediate, and upper limits of the viscosity ranges were used. With the Saybolt Furol instrument the determinations were made at the temperatures specified for the different cutbacks, *i.e.* at 50°, 60°, and 82° C. With the Standard tar viscometer, determinations were made at 25° C for the R.C. and M.C. 1, 2, 3 series and at 40° C for the R.C. and M.C. 4 and 5 series. These are the temperatures normally used with this instrument for cutback bitumens. The Saybolt Furol viscometer has a small orifice of 3·15 mm diameter, thus necessitating test temperatures up to 82° C, whereas the Standard tar viscometer has an orifice of 10 mm diameter, except for testing very fluid materials when an orifice of 4 mm diameter is used. The lower test temperatures (25° and 40° C) that can be used with the Standard tar viscometer minimize the possibility of loss of volatiles during the test.

The results given by the Saybolt Furol viscometer, when plotted on a log–log scale against the corresponding results by the Standard tar viscometer, lie approximately on a straight line. From the slope of this line the equivalent range of the Standard tar viscometer corresponding to the range of the Saybolt Furol viscometer was obtained for each grade of cutback, the upper limit for each grade being approximately three times the value of the lower limit, as shown in Table I.

TABLE I

Table of Comparative Results

R.C. and M.C. grade	Saybolt Furol viscosity range(s)	Approximate equivalent S.T.V. range(s)
1	75–150 at 50° C	50–150 at 25° C (4-mm orifice)
2	100–200 at 60° C	7– 20 at 25° C (10-mm orifice)
3	250–500 at 60° C	25– 75 at 25° C (10-mm orifice)
4	125–250 at 82° C	14– 45 at 40° C (10-mm orifice)
5	300–600 at 82° C	60–200 at 40° C (10-mm orifice)

A more precise method of conversion is not possible, because the tests are carried out at different temperatures, and because bitumens made from different crudes do not all soften equally when heated. Bitumens from waxy crudes have a particularly high susceptibility to temperature change. Because of this, and because they show some crystallization at lower temperatures, viscosity conversion figures for such bitumens are exceptional. Standard tar viscosity tests on a series of cutbacks made from a waxy crude showed equivalent viscosities which were generally 25 to 50 per cent higher than those quoted in Table I.

The necessity for this work provides a typical example of the desirability for closer international relations which will lead to the adoption of the same arbitrary standard tests for measuring the flow properties of bituminous materials.

ACKNOWLEDGMENT

The work described above was carried out as part of the programme of the Road Research Board of the Department of Scientific and Industrial Research, and is published by permission of the Director of Road Research.

* MS received 24 August 1953.

† Road Research Laboratory, Department of Scientific and Industrial Research.

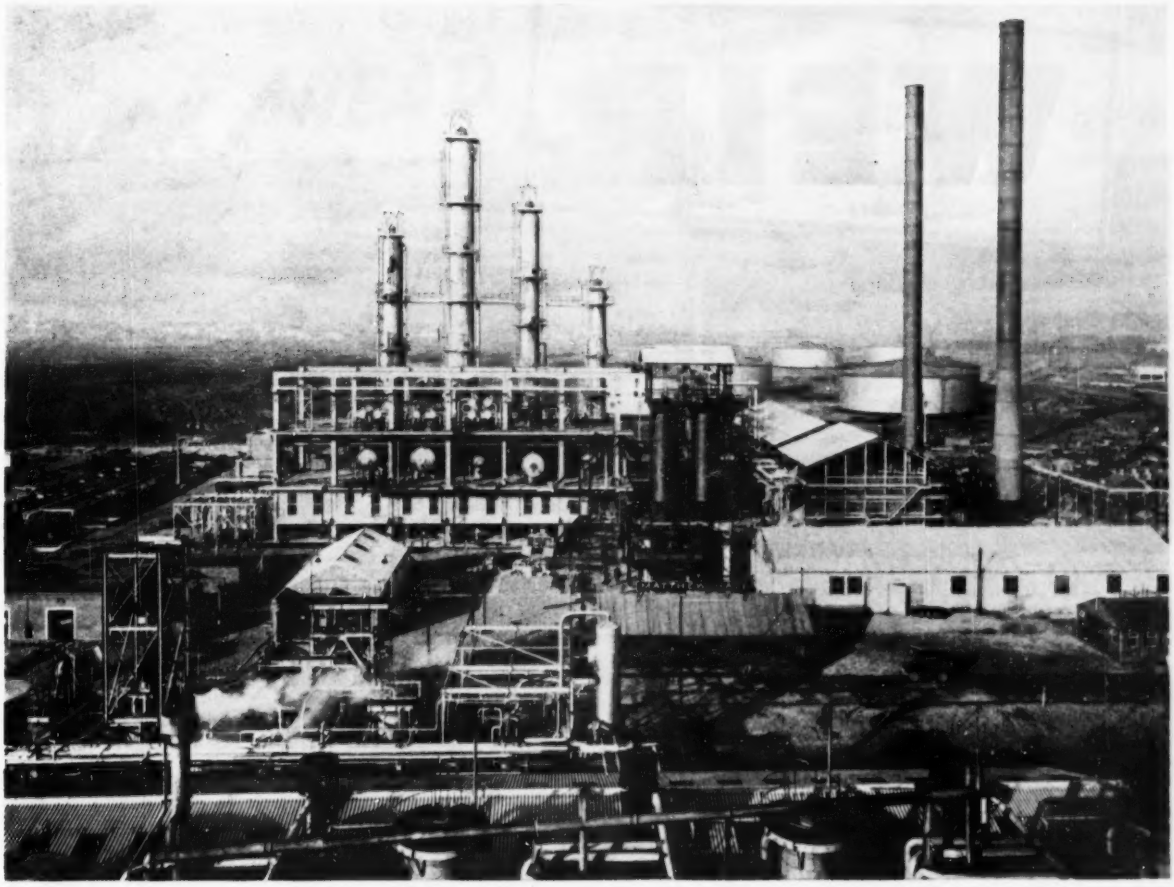

THE

MATTHEW HALL

GROUP OF COMPANIES

ESTD. 1848

MATTHEW HALL

OIL REFINERY, CHEMICAL AND INDUSTRIAL ENGINEERS

ERECTION OF PLANT AND MACHINERY

WELDED OIL PIPE LINES

FLAMEPROOF ELECTRICAL INSTALLATIONS

THE MATTHEW HALL GROUP OF COMPANIES

MATTHEW HALL & CO. LTD. MATTHEW HALL (PTY.) LTD.
KELCO (METALS) LTD. GARCHEY LTD.

LONDON . . . 26-28 Dorset Square, N.W.1	JOHANNESBURG . 52 Commissioner Street	DUBLIN . . . . . 29 Westland Row
MANCHESTER . . . . 95-97 Princess Street	GERMISTON . . . . . Wadeville	WEST INDIES . . . . . Kingston, Jamaica
GLASGOW . . 88 & 91 Dykehead Street, E.2	DURBAN . . . . . 100-102 Williams Road	GIBRALTAR . . . . . P.O. Box 266
BELFAST . . . . . Greenwood Avenue	CAPE TOWN . . . . . Riebeeck Square	BULAWAYO . . . . . Abercorn House
	WELKOM . . . . . Third Street	

WEIR

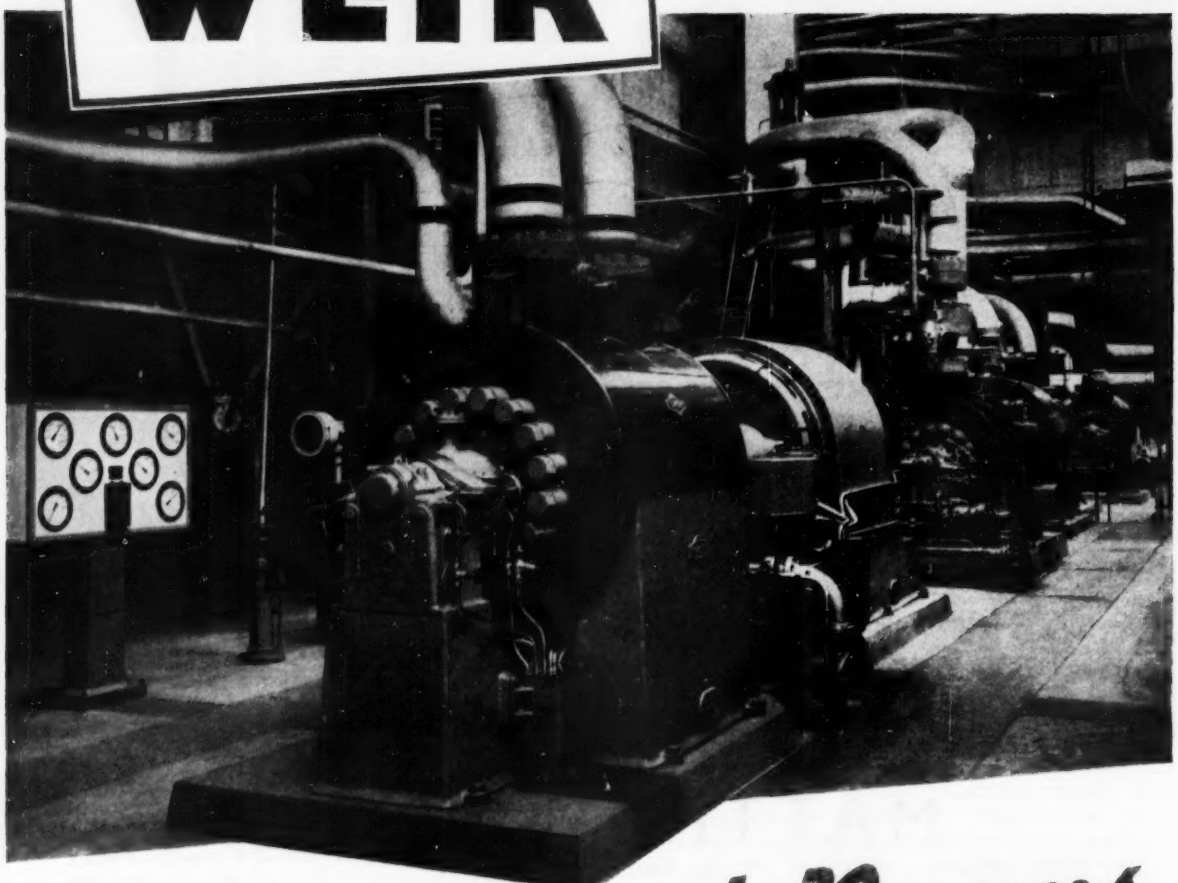

Boiler Feed Pumps

in single and multi-stage designs for the highest temperatures and pressures. Turbine and electrically driven pumps in ring section or barrel casing designs of the highest efficiency.

G. & J. WEIR LTD.
CATHCART : GLASGOW

FEED HEATERS · DE-AERATORS · REGENERATIVE CONDENSERS
EVAPORATING & DISTILLING PLANTS · HEAT EXCHANGERS

LOOK AHEAD

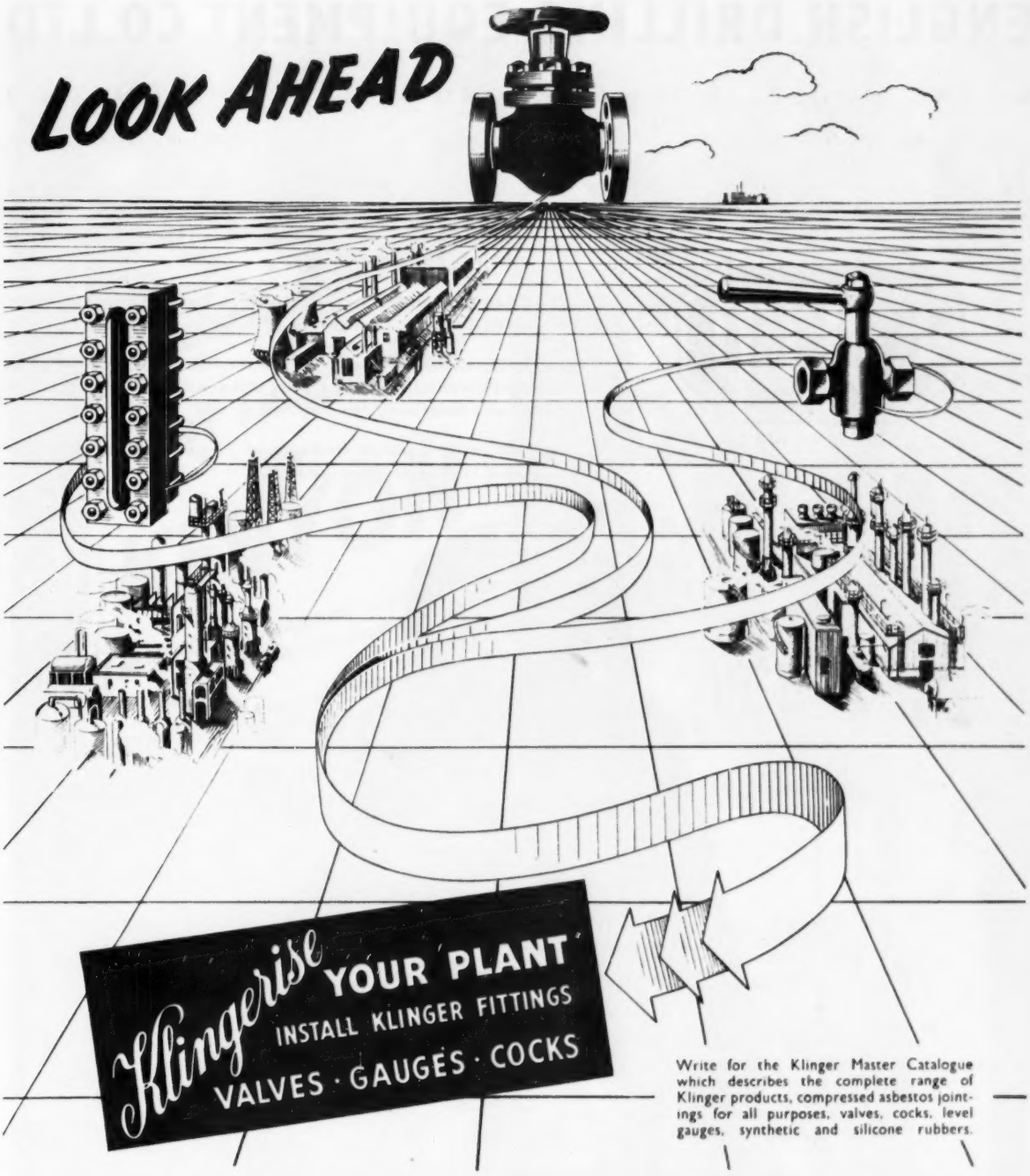

Klingerise YOUR PLANT
INSTALL KLINGER FITTINGS
VALVES · GAUGES · COCKS

Write for the Klinger Master Catalogue which describes the complete range of Klinger products, compressed asbestos jointings for all purposes, valves, cocks, level gauges, synthetic and silicone rubbers.

RICHARD KLINGER LIMITED, KLINGERIT WORKS, SIDCUP, KENT, ENGLAND

Manufacturing Licensees for Canada — Agents throughout the World — Manufacturing Licensees for U.S.A.

JOSEPH ROBB & COMPANY, LIMITED
5575, COTE ST. PAUL ROAD, MONTREAL, 20, CANADA
Telephone: WILBANK 3181 Cable: ROBCO
Branches at: SYDNEY, N.S., HALIFAX, N.S., OTTAWA, Ont., TORONTO, Ont., HAMILTON, Ont., WINNIPEG, Man., EDMONTON, Alta., VANCOUVER, B.C.

THE KLINGER CORPORATION OF AMERICA
95, RIVER STREET, HOBOKEN, NEW JERSEY, U.S.A.
Telephone: HOBOKEN 2-7915 Cable: KLINGDALE
New York Office: 17, BATTERY PLACE, NEW YORK 4, N.Y., U.S.A.
Telephone: WHITEHALL 3-8996 Cable: COFFDALE

ENGLISH DRILLING EQUIPMENT CO LTD

BILBAO HOUSE, 36–38 NEW BROAD STREET, LONDON, E.C.2

Telephone: LONdon Wall 4941–4 **Telegrams: Bullwheel, Ave, London**

EDECO

REGD. TRADE MARK

The Edeco Twin Jet Bit is recommended for use in conjunction with high velocity drilling fluid circulation. The cuttings are swept upwards by the jet stream, keeping the bottom of the hole clean, allowing FASTER PENETRATION and MORE HOLE per bit.

The Edeco Twin Jet Bits are available with all the cutter designs illustrated in the EDECO Rock Bit Catalogue No. 82.

The Jet Circulation ways are forged into the body of the bit avoiding the necessity for separate Tubes and allowing thicker walls around the circulation passages and, consequently, less danger of "cut outs".

The outlets of these passages are fitted with Tungsten Carbide Nozzles with bore size to suit customer's requirements.

TWIN JET

TYPE VS

SUBSIDIARY COMPANIES

EDECO PROSPECTORS LTD
Baribу Works, Lindley Moor Road,
Nr. Huddersfield, Yorks.
Telephone: Elland 2876 7

EDECO CANADA LTD
10103–80th Avenue,
Edmonton, Alberta.
Telephone: Edmonton 35825

EDECO GERMANY G.M.B.H.
Folschblock C, Hermannstr. 40,
Hamburg, 1.
Telephone: Hamburg 33 39 67

EDECO (TRINIDAD) LTD
P.O. Box 27, San Fernando,
Trinidad, B.W.I.
Telephone: San Fernando 2819

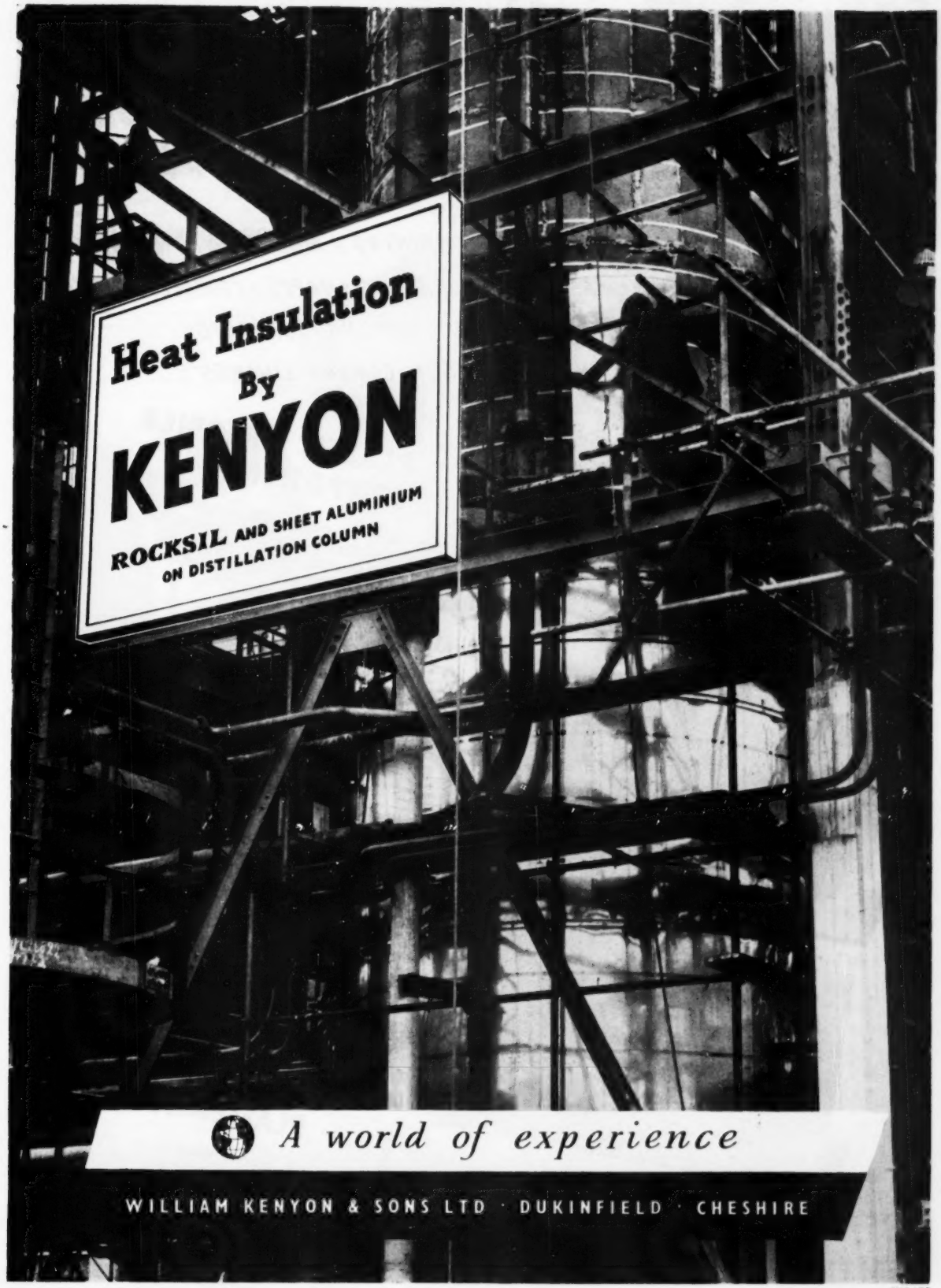
Heat Insulation
By
KENYON
ROCKSIL AND SHEET ALUMINIUM
ON DISTILLATION COLUMN
A world of experience
WILLIAM KENYON & SONS LTD · DUKINFIELD · CHESHIRE

KH 158

DURAX

THE INDISPENSABLE REFRACTORY!

- ★ RAMMING PATCHING & MONOLITHIC LININGS
- ★ SPECIAL & EMERGENCY SHAPES · COMPLETE LININGS
- ★ THIN SOUND & STRONG JOINTING
- ★ PNEUMATIC GUN CEMENT LININGS

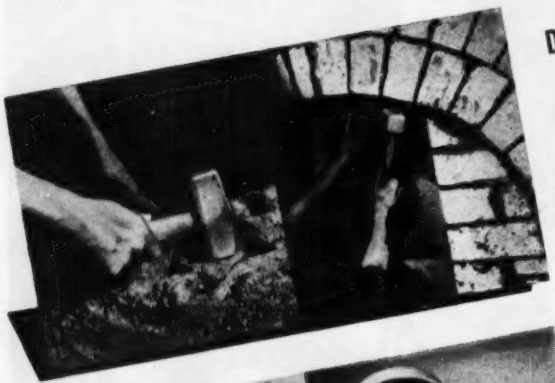

DURAX No 1 PLASTIC FIREBRICK COMPOSITION

Supplied ready mixed for immediate use. Suitable for rammed linings and patching existing Durax No. 1 or firebrick linings. Service temperature range 1300/1650°C.

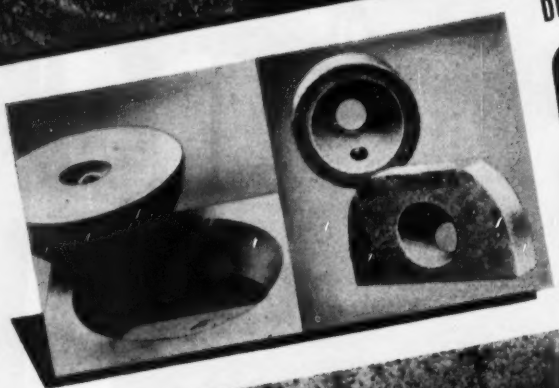

DURAX No 2 REFRACTORY CONCRETE

For casting in situ and making special shapes. Supplied dry. Special characteristics include—rapid setting as hard as firebrick: pours into position: no permanent volume change: little tendency to spall. Maximum service temperature 1300°C.

DURAX No 3 REFRACTORY CEMENT

A finely ground air setting cement for jointing all types of firebricks. Supplied dry. Special characteristics include—produces thin and strong joints: negligible shrinkage: highly refractory: economical in use. Maximum service temperature 1650°C.

DURAX No 5 GUNNING OR PLASTERING CEMENT

A cement designed for application with a pneumatic gun. Alternatively it may be plastered into position. Durax No. 5 has little rebound loss when applied by gun to Catalytic Regenerators and forms a dense tough lining with a maximum service temperature of 1300°C.

★ *Fully descriptive literature on all of these grades of Durax is available on request*

GENERAL REFRACTORIES LTD

GENEFAX HOUSE · SHEFFIELD 10 Telephone SHEFFIELD 31113

284

BABCOCK

Refinery Equipment

Right: Fusion-welding the longitudinal seam of a pressure vessel at the Renfrew works of Babcock & Wilcox, Ltd.

Below: Routine X-ray examination, applied to every inch of weld, shows less than 10 inches defective in every *mile*.

BOILERS

WELDED PRESSURE VESSELS

HEAT EXCHANGERS

WASTE-HEAT UTILIZATION PLANT

CRANES

The picture above symbolises an experience of over 20 years in the manufacture of fusion-welded pressure vessels, a process that was pioneered by Babcock & Wilcox and developed by them to its present state of perfection.

The operator is supervising the automatic welding of a longitudinal seam in a large pressure vessel—maybe the high-pressure drum of a Babcock boiler, a high-pressure manifold or part of a large treating tower destined for one of the world's new oil refineries, many of which have Babcock equipment.

With 75 years of boilermaking experience, including their 23 years development of the fusion-welding process for the manufacture of pressure vessels, Babcock & Wilcox are outstandingly well equipped to meet the demands of the oil industry for complete modern steam-raising plants, treating towers, high-pressure manifolds, heat exchangers and plant for the utilization of waste heat.

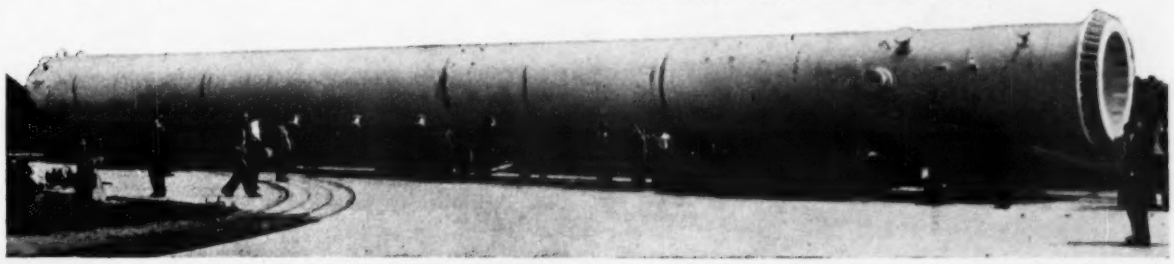

BABCOCK & WILCOX LTD · BABCOCK HOUSE · FARRINGDON STREET · LONDON · E.C.4

Tubes and Plates for Heat Exchangers

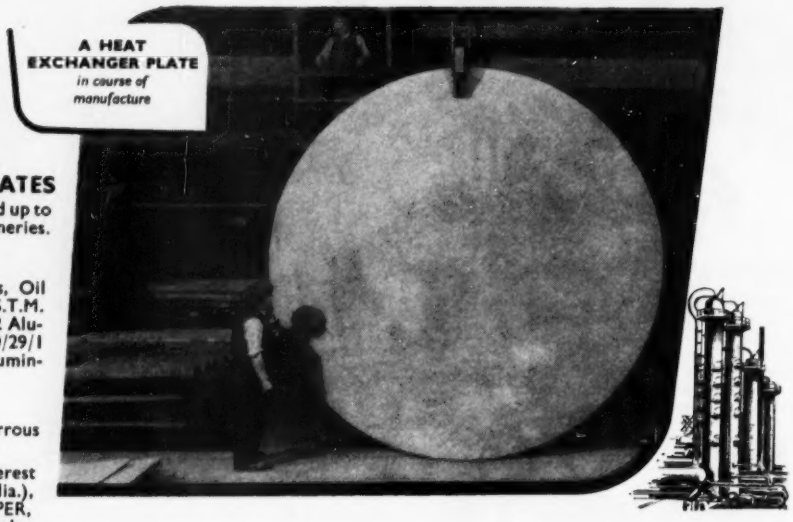

A HEAT EXCHANGER PLATE *in course of manufacture*

Birmingham Battery "True to Specification" products in non-ferrous metals are widely used in the Oil Industry.

"BATTERY" CONDENSER PLATES
in Naval Brass or Yellow Metal are produced up to the heaviest sizes required by the Oil Refineries.

CONDENSER TUBES
for Heat Exchangers, Steam Condensers, Oil Coolers etc., to British Standard and A.S.T.M. Specifications in—"BATALBRA" (76/22/2 Aluminium Brass), Admiralty Mixture (70/29/1 Brass), 70/30 Brass, Cupro-Nickel and Aluminium Bronze.

BI-METAL TUBES
for combining the properties of Non-Ferrous Tubes with Steel Tubes.

- Other "BATTERY" manufactures of interest to the Oil Industry are TUBES (up to 24" dia.), SHEETS, STRIP, ROD and WIRE in COPPER, BRASS, PHOSPHOR-BRONZE etc., to the latest British Standard Specifications. Where necessary, we should be pleased to work to customers' own requirements.

CONTRACTORS TO LEADING OIL COMPANIES

The BIRMINGHAM BATTERY and METAL CO LTD
SELLY OAK BIRMINGHAM 29
Over a Century of Independent Enterprise

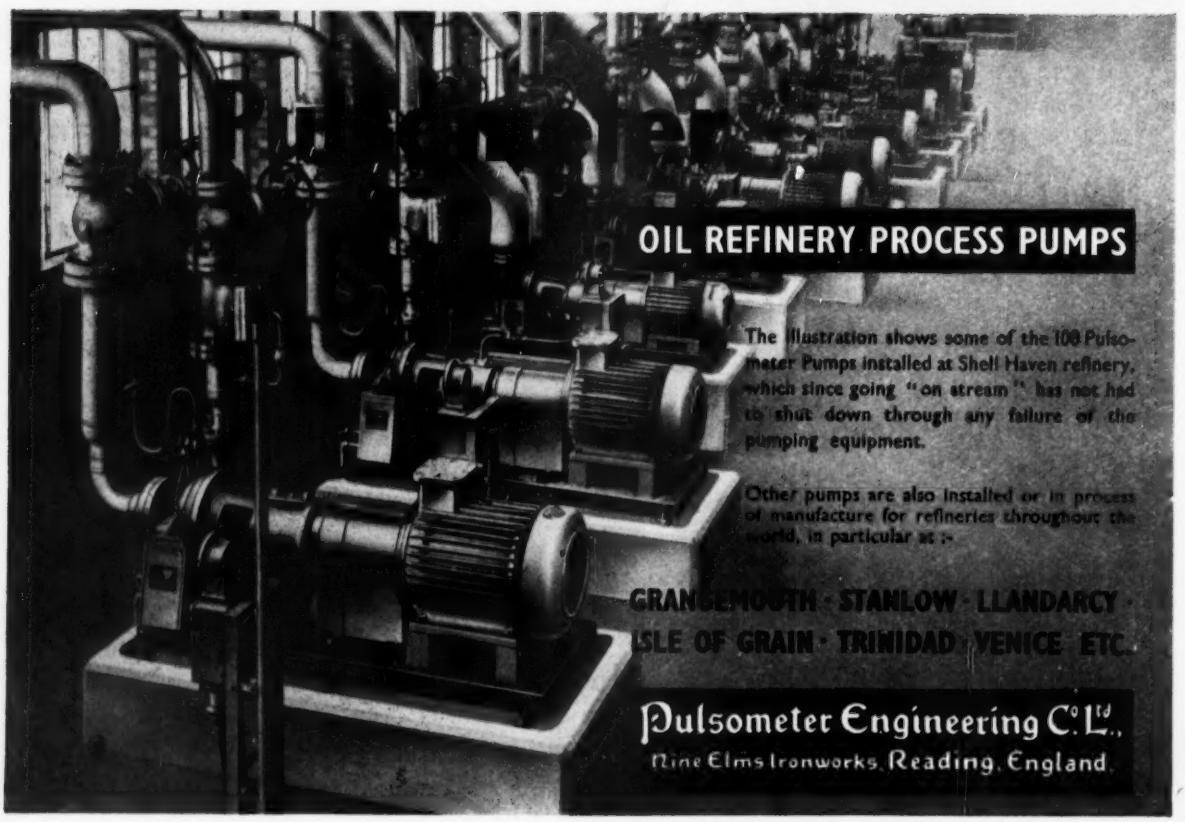

OIL REFINERY PROCESS PUMPS

The illustration shows some of the 100 Pulsometer Pumps installed at Shell Haven refinery, which since going "on stream" has not had to shut down through any failure of the pumping equipment.

Other pumps are also installed or in process of manufacture for refineries throughout the world, in particular at :-

GRANGEMOUTH · STANLOW · LLANDARCY · ISLE OF GRAIN · TRINIDAD · VENICE ETC.

Pulsometer Engineering Co. Ltd.
Nine Elms Ironworks, Reading, England.

Quasi-Arc

open the most advanced Arc Welding Research Establishment in the Commonwealth

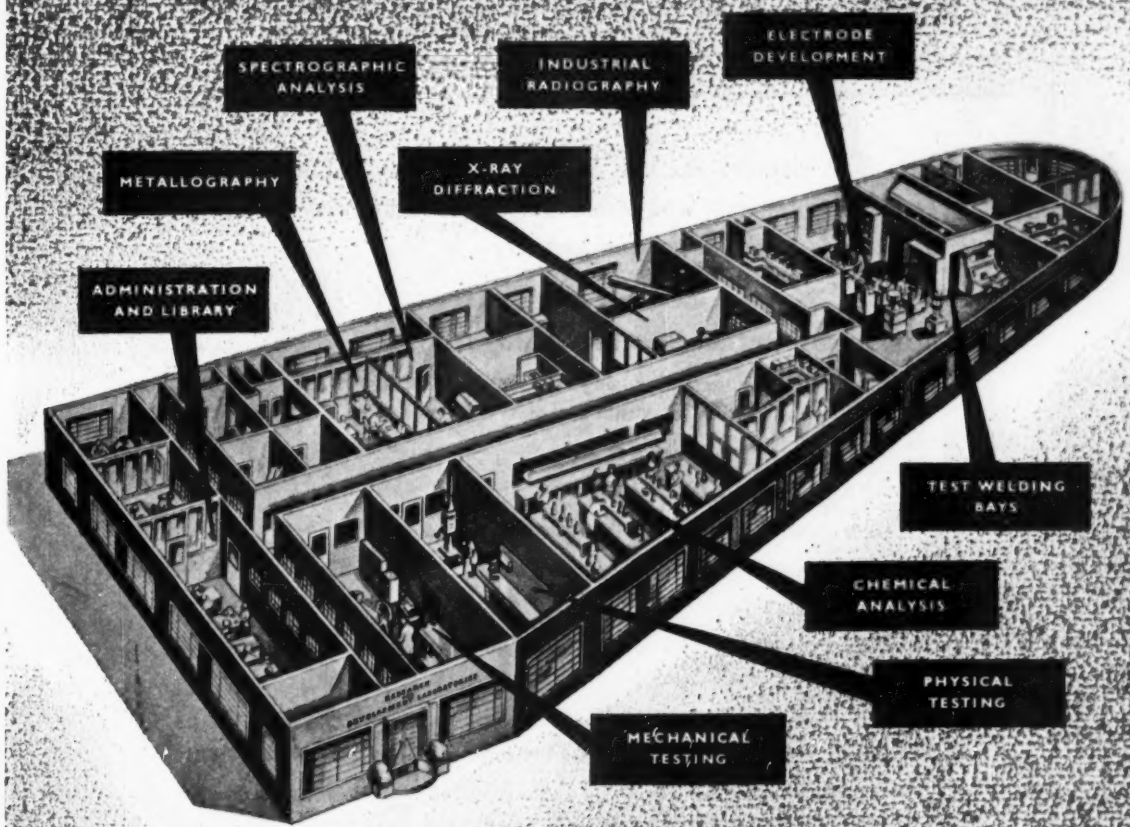

Here are some of the new and improved electrodes produced by Quasi-Arc Research:

Victor—Mild Steel type specifically designed for welding inclined and vertical joints by the vertically downwards method—faster, easier depositing, smooth welds, negligible slag cleaning.

Vortic—(Molybdenum Bearing)—for welding low alloy high tensile steels—especially for creep resistance.

Both **Victor** *and* **Vortic** *(Molybdenum Bearing) are approved by Lloyd's and the Ministry of Transport, and conform to B.S. 639: 1952.*

Duroid No. 1 (New Type)—for hard surfacing; 250 V.P.H. hardness in weld metal.

Duroid No. 2 (New Type)—for hard surfacing; 350 V.P.H.

Duroid No. 3 (New Type)—for hard surfacing; 700 V.P.H.

Manganoid (New Type)—for reinforcing 12/14% manganese steel. 250 V.P.H. in the weld metal, work hardening to 500 V.P.H.

Duroid *Nos. 1, 2 and 3 and* **Manganoid**—*as redesigned, provide easy application, neat deposit, easy slag removal, equal to the best types of Mild Steel electrodes.*

Ferroloid No. 1 (New Type)—for machinable welds in cast iron without preheating. An improved electrode with quiet smooth arc and easy slag control.

Ferroloid No. 2 (New Type)—an improved steel-cored electrode for strength welds in cast iron.

Alumoid No. 2 (New Type)—fully extruded electrode for welding aluminium silicon alloys. Robust and easier depositing. Approved by the Ministry of Supply.

THE QUASI-ARC COMPANY LIMITED HILTON, STAFFORDSHIRE

MANUFACTURERS OF ELECTRODES, PLANT AND ACCESSORIES FOR ELECTRIC ARC WELDING

QA 43

IS YOUR PETROLEUM BOOKSHELF COMPLETE?

It is if it includes ALL the books listed below. Each one is essential to the man who wants to keep abreast of developments and trends in the petroleum industry

● **Reviews of Petroleum Technology** **VOLUME 13**

Surveying developments during 1951, this volume brings the wide field of petroleum literature within the covers of one book. Price 50s.

● **Oil Shale and Cannel Coal**

Eight hundred pages of the latest data on all aspects of oil from shale. Price 63s.

● **Electrical Code**

Covers safety practices in the use of electricity in the field, refinery and storage installation. Price 26s.

● **ASTM/IP Petroleum Measurement Tables** **BRITISH EDITION**

Authoritative tables for use in computing oil quantities in territories which employ the British system of weights and measures. Price 50s.

● **Petroleum Measurement Manual**

A companion Volume to the "Tables." Essential to anyone who has to deal with the sampling and measurement of liquid petroleum products. Price 25s.

All the above books can be obtained through a bookseller or direct from

THE INSTITUTE OF PETROLEUM
26 PORTLAND PLACE, LONDON, W.1

Specialists in the Manufacture of Laboratory Apparatus for Testing Petroleum Products

I.P. Centrifuge

I.P. Viscometers

I.P. Bromine Number Apparatus

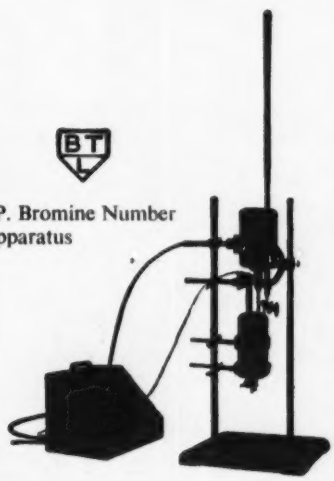

I.P. Flash and Fire Point Apparatus

A full range of apparatus to I.P. specifications

BAIRD & TATLOCK (LONDON) LTD.

Scientific Instrument Makers

FRESHWATER ROAD, CHADWELL HEATH, ESSEX

Crude Atmospheric and Vacuum Distillation Unit

Designed by Foster Wheeler for the Vacuum Oil Company's Refinery at Coryton.

FOSTER WHEELER *London New York and Paris*

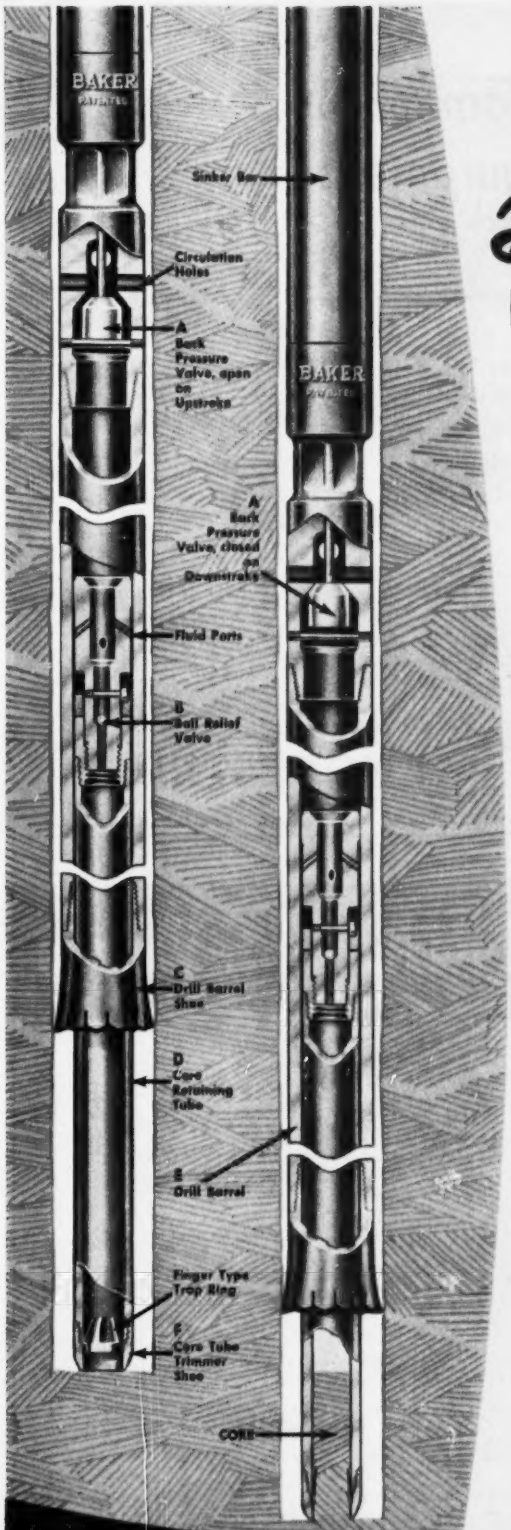

attention!

CABLE TOOL OPERATORS

WHEN YOU WANT CORES that are a true, uncontaminated, maximum size sample of the formation, at low cost, nothing can equal the BAKER CABLE TOOL CORE BARREL.

This efficient coring device not only meets the requirements of the geologist, but also is extremely popular with both operator and crew because of its simplicity of operation, and its "holemaking" ability. There are no complicated adjustments, and any experienced cable tool driller can *secure good cores* and *maximum footage right from the start.*

Coring with a Baker Cable Tool Core Barrel is extremely economical, with operating and maintenance costs held to a minimum. With proper care, this Core Barrel will last indefinitely, and replacement or re-building of the few wearing parts is necessary only after prolonged service.

Advantages of Coring with the Baker Cable Tool Core Barrel

Cores up to 2 15/16" in diameter, and up to 7 feet in length are readily taken from a wide variety of formations.

The accurate, uncontaminated cores eliminate danger of passing through low-pressure sands that might prove productive.

Tests for porosity, saturation and permeability can be made without difficulty, and *positive proof* of the *exact character* of any sand is ensured. And all of these advantages are secured with little loss of drilling time, as a Baker Cable Tool Core Barrel takes perfect cores at a speed comparable with straight drilling.

Strong and Long Lasting—Easy to Operate

The sturdy construction consists of an outer Drill Barrel (E) and an inner Core Retaining Tube (D). The Trimmer Shoe (F) remains in contact with the formation until the core is taken, after which the entire Core Barrel (with core intact) is removed from the well.

The Drill Barrel (E) slides along the Core Retaining Tube (D) and cuts away the formation, thus permitting the Core Retaining Tube to follow down over the undisturbed core and secure a true sample of the formation.

Features which assist in taking good cores include: the Ball Check Valve (B) which permits escape of water entrapped in the Core Retaining Tube so that fluid under pressure never acts on the core; also, the Back Pressure Valve (A) which closes on the downstroke so that water in the annulus between the two Barrels is driven downward with sufficient force to keep the teeth of the Drill Barrel Shoe (C) free from cuttings.

ANY BAKER REPRESENTATIVE, or office, can furnish additional details on this efficient, low-cost Core Barrel, which provides many advantages in cable tool drilling.

BAKER OIL TOOLS, INC.

HOUSTON • LOS ANGELES • NEW YORK

BAKER Product No. 820 **CABLE TOOL CORE BARREL**

DORMAN

Flameproof equipment

(BUXTON CERTIFIED)

Flameproof prismatic lighting fitting, the DORMAN "DIOPRISM" 100 watt – conforms to requirements of the Ministry of Mines.

4-way S.P. & N. Flameproof switch fuse distribution board —

— with "T" type isolating switch

DORMAN & SMITH LTD. **MANCHESTER 5**

The Pioneers of Tower Packing

THE HYDRONYL SYNDICATE LTD.

14 GLOUCESTER RD., LONDON, S.W.7

Telephone: WEStern 4744 Telegrams: HYDRONYL • KENS • LONDON

TRIANGLE Valves

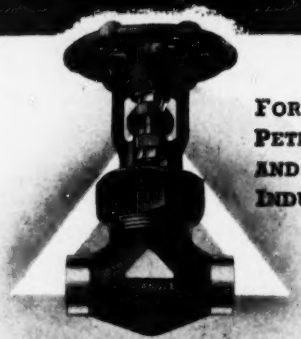

FOR THE PETROLEUM AND ALLIED INDUSTRIES

FORGED STEEL GATE VALVE

FORGED STEEL

Screwed Ends. Sizes ¼" to 2". Pressures from 150 to 1500 lbs. per sq. in.

Flanged Ends. Sizes ¼" ⅜" 1" & 1½". Pressures 150, 300 & 600 lbs. per sq. in.

CAST STEEL

Flanged Ends. Sizes 2" to 12". Pressures 150, 300 & 600 lbs. per sq. in.

TRIANGLE VALVE CO. LTD.

Phone: 82631 (6 lines) Telegrams & Cables: TRIVALVE, WIGAN

LAMBERHEAD GREEN - WIGAN - ENGLAND

"Corronel B" is the latest addition to the Wiggin range of high-nickel alloys. A nickel-molybdenum-iron alloy, it is of particular interest because of its exceptional resistance to most acids (but especially hydrochloric acid in any strength and at any temperature—including boiling). It has already been tested and proved in service and is now available in this country in wrought form.

A publication giving detailed properties of CORRONEL B is available free of charge

* *Trade Mark*

HENRY WIGGIN & COMPANY LIMITED
WIGGIN STREET · BIRMINGHAM · 16

CRAIG

COMPREHENSIVE SERVICE

*

REFINERY DESIGN AND CONSTRUCTION

•

ATMOSPHERIC AND
VACUUM DISTILLATION UNITS

•

COMBINED DISTILLATION,
CRACKING, REFORMING AND
VAPOUR PHASE TREATING UNITS

•

PARAFFIN WAX EXTRACTION,
REFINING AND MOULDING

•

GASOLINE RECOVERY
AND STABILISATION UNITS

•

HEAT EXCHANGE EQUIPMENT OF ALL TYPES

•

FRACTIONATING COLUMNS
AND TUBE STILLS

A.F. CRAIG & COMPANY LTD

CALEDONIA ENGINEERING WORKS

PAISLEY SCOTLAND

London Office: 727, Salisbury House, London Wall, E.C.2.

Telephone: MONARCH 4756

C/S